SMITHSONIAN CONTRIBUTIONS TO THE EARTH SCIENCES • NUMBER 10

Mineralogy, Mineral-Chemistry, and Composition of the Murchison (C2) Meteorite

Louis H. Fuchs, Edward Olsen, and Kenneth J. Jensen

SMITHSONIAN INSTITUTION PRESS
City of Washington
1973

ABSTRACT

Fuchs, Louis H., Edward Olsen, and Kenneth J. Jensen. Mineralogy, Mineral-Chemistry, and Composition of the Murchison (C2) Meteorite. *Smithsonian Contributions to the Earth Sciences,* number 10, 39 pages, 19 figures, frontispiece, 1973.—The Murchison meteorite shower, September 28, 1969, occurred in and around Murchison, Victoria, Australia. Chemical and mineralogical analyses established it as a type II carbonaceous chondrite (C2). Murchison consists largely of fine-grained black matrix which has been identified as primarily a mixture of two iron-rich, low-aluminum chamosite polytypes. Contained in the matrix are four main types of inclusions: (1) single crystals and crystal fragments, (2) loosely aggregated clusters of crystals ("white inclusions"), (3) discrete true chondrules, (4) xenolithic fragments of two other meteorite types (mostly a unique kind of C3 chondrite).

The first type of inclusions consists of unzoned and highly zoned olivines, unzoned (disordered and ordered) orthopyroxenes, clinoenstatite, and rare diopside. Prominent minor phases are calcite, chromite, metal (with occasional traces of schreibersite), troilite, pentlandite, and two phases that could not be fully characterized.

The second type of inclusions consists primarily of grains of olivine (Fa 0 to Fa 40), lesser low-Ca pyroxenes, and minor spinel, calcite, whewellite, hibonite, perovskite, chromite, pentlandite, and rare Ca-pyroxene.

The true chondrules consist of olivine, Ca-poor pyroxene, occasional metal, and, in rare instances, one of the poorly characterized phases. The chondrules are not texturally typical of the ordinary chondrites, but resemble more closely those chondrules seen in C3 and C4 chondrites.

The fourth type of inclusion consists mainly of distinct xenolithic fragments of a light blue-gray chondrite type that resembles certain C3 chondrites (like Vigarano), though not in all aspects. These xenolithic fragments consist of disequilbrated olivines and pyroxenes, abundant pentlandite and troilite, and virtually no metal. In addition, a single xenolithic fragment was found of an unknown meteorite type.

Ca- and Al-rich glasses (of varying compositions) are found as blebs, with or without gas bubbles, contained within olivine crystals. The average Ca/Al ratio of these glasses approximates that for all meteoritic matter. They may represent early (nonequilibrium) subcooled condensates from the solar nebula. This nonequilibrium stage was apparently followed by equilibrium condensation through intermediate to low temperatures at which the layer-lattice phases condensed in abundance and incorporated crystals and fragments of the higher temperature phases.

OFFICIAL PUBLICATION DATE is handstamped in a limited number of initial copies and is recorded in the Institution's annual report, *Smithsonian Year.* SI PRESS NUMBER 4784. SERIES COVER DESIGN: Aerial view of Ulawun Volcano, New Britain.

Library of Congress Cataloging in Publication Data
Fuchs, Louis H.
Mineralogy, mineral-chemistry, and composition of the Murchison (C2) meteorite.
(Smithsonian contributions to the earth sciences, no. 10)
I. Meteorites. I. Olsen, Edward John, 1927—joint author. II. Jensen, Kenneth J., joint author. III. Title. IV. Series: Smithsonian Institution. Smithsonian contributions to the earth sciences, no. 10.
QE1.S227 no. 10 [QE395] 550'.8s [523.5'1] 72-13427

For sale by the Superintendent of Documents, U.S. Government Printing Office, Washington, D.C. 20402
Price 75 cents domestic postpaid or 55 cents GPO Bookstore

Contents

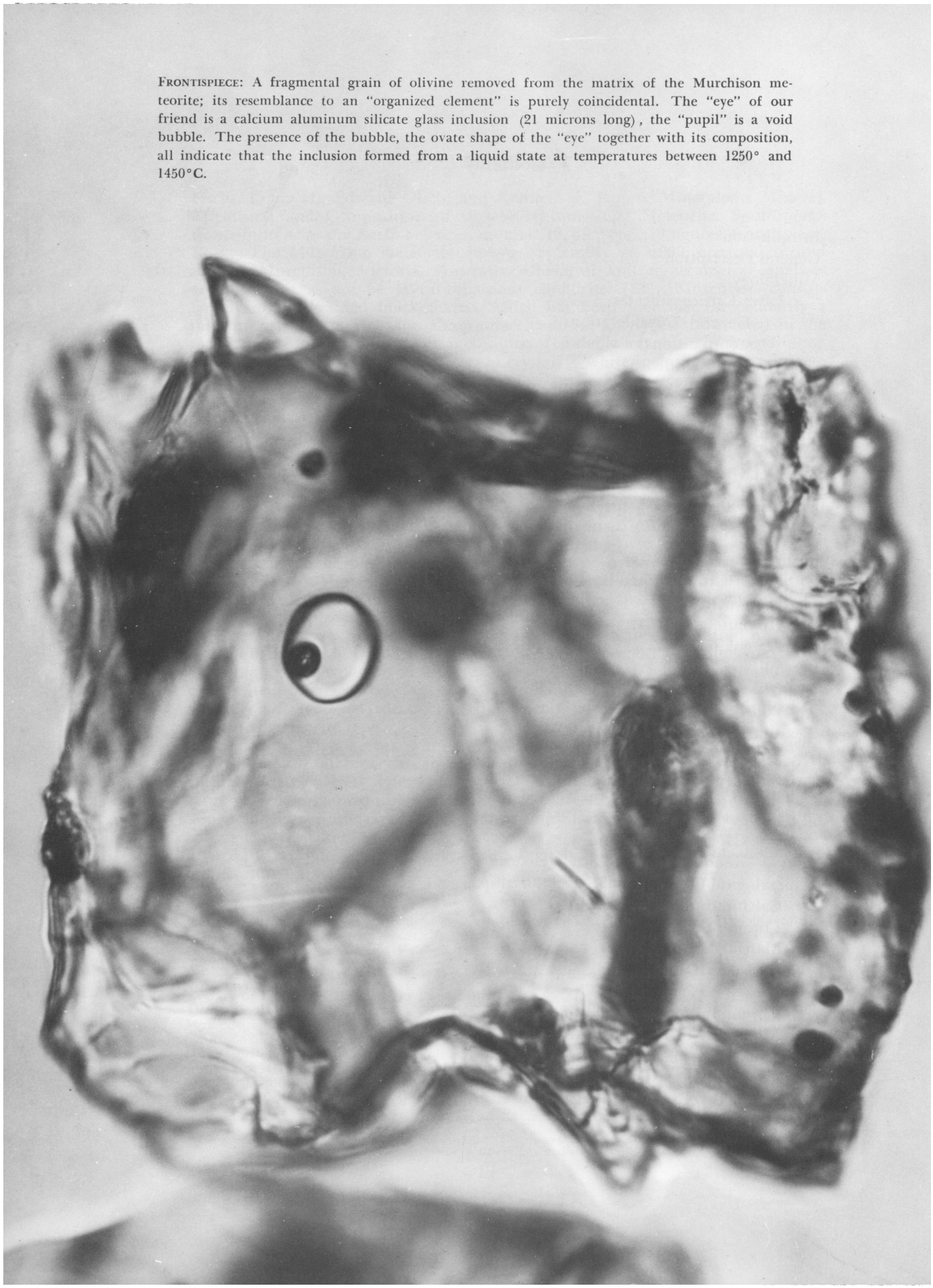

FRONTISPIECE: A fragmental grain of olivine removed from the matrix of the Murchison meteorite; its resemblance to an "organized element" is purely coincidental. The "eye" of our friend is a calcium aluminum silicate glass inclusion (21 microns long), the "pupil" is a void bubble. The presence of the bubble, the ovate shape of the "eye" together with its composition, all indicate that the inclusion formed from a liquid state at temperatures between 1250° and 1450°C.

Mineralogy, Mineral-Chemistry, and Composition of the Murchison (C2) Meteorite

Louis H. Fuchs, Edward Olsen, and Kenneth J. Jensen

Introduction

The Murchison meteorite shower occurred on September 28, 1969, 1045 hours local time, 85 miles north of Melbourne, Australia. Details of the fall and an initial description are given by Lovering et al. (1971). In addition, Clarke (personal communication) has assembled details pertinent to the strewnfield. A chemical analysis was reported by Jarosewich (1971) and a short description was published by Ehmann et al. (1970). A somewhat more detailed description was given by Fuchs, Jensen, and Olsen (1970) before the 1970 meeting of the Meteoritical Society.

Murchison is the largest known fall of a type II carbonaceous chondrite. The major portion, approximately 65 kg., is located at the Field Museum of Natural History, Chicago. Other major portions are located at the National Museum of Natural History, Smithsonian Institution, Washington, D.C. (approximately 30 kg), the Australian Museum, Sydney (approximately 4 kg), and the University of Melbourne (approximately 7 kg). In addition, smaller quantities, up to several kilograms, have been acquired around the world by a number of museums, universities, and private persons.

In making this study we were fortunate in having such a large quantity of this meteorite available. Several hundred hand specimens were examined and seven polished microscope mounts were used. Mineral identifications were made by optical examination of handpicked grains and confirmed by X-ray powder diffraction in all instances.

ACKNOWLEDGMENTS.—We would like to thank Dr. Milton Blander, Argonne National Laboratory, for many stimulating discussions on some of the features observed in the Murchison meteorite and Dr. E. Roedder, U.S. Geological Survey, for his penetrating comments on portions of the manuscript. We are grateful to members of the staff of the National Museum of Natural History: Dr. Brian Mason, Eugene Jarosewich, Joseph Nelen, Grover Moreland, and Roy S. Clarke, Jr., for helpful counsel and for making available unpublished data on Murchison. Dr. Warren Forbes and Mrs. Margaret Meyers, University of Illinois—Chicago Circle Campus, helped in a portion of the microprobe work and data reduction, and this is gratefully acknowledged. We thank Mr. Karl Anderson, Argonne National Laboratory, for help on the microprobe at ANL, and Irene M. Fox (ANL) and Ralph W. Bane (ANL) who obtained the carbon,

Louis H. Fuchs, Chemistry Division, and Kenneth J. Jensen, Chemical Engineering Division, Argonne National Laboratory, Argonne, Illinois 60439; Edward Olsen, Field Museum of Natural History, Chicago, Illinois 60605 and Department of Geological Sciences, University of Illinois–Chicago Circle, Chicago, Illinois 60680.

hydrogen, and nitrogen data reported. We especially thank Mr. Francis (Bert) Eliason of Murchison, Australia, for making available the most significant portion of the Murchison fall and pointing out features we might otherwise have missed, and Mr. Glenn Commons and Mr. R. Groh who provided the financial assistance to obtain the major portion of this significant meteorite. Edward Olsen was partly supported by a grant from the National Aeronautics and Space Administration (NGR–014–052–001), and Louis H. Fuchs was partially supported by a NASA research grant. This grant is gratefully acknowledged. Part of the work was supported under the auspices of the United States Atomic Energy Commission. The cost of publication was paid by Argonne National Laboratory and the Field Museum of Natural History.

General Description

Murchison consists of numerous individuals ranging from a few grams to seven kilograms. Most of the pieces are surrounded by fusion crust; however, because of low mechanical strength many are broken and cracked, some possessing no crust at all because it has spalled off at impact and afterward due to normal handling. Many specimens show severe desiccation cracking, presumably due to loss of volatiles. Several observers have noted gradual weight changes, both losses and gains, that are presumably due to changes in atmospheric conditions in the several laboratories where weight checks were made. Fine-grain size coupled with good porosity and permeability permit the meteorite to "breathe." Although this has only modest effects in the mineralogy, major composition, and petrography, it can have serious implications for any work that involves gases and organic chemistry.

In comparing hand specimens with other C2 chondrites Murchison shows a similarity only to Murray. The ratio of inclusions + chondrules to black matrix is clearly higher in both these meteorites (Figure 1) in contrast to others of this group, such as Mighei, Cold Bokkeveld, etc. Typical of

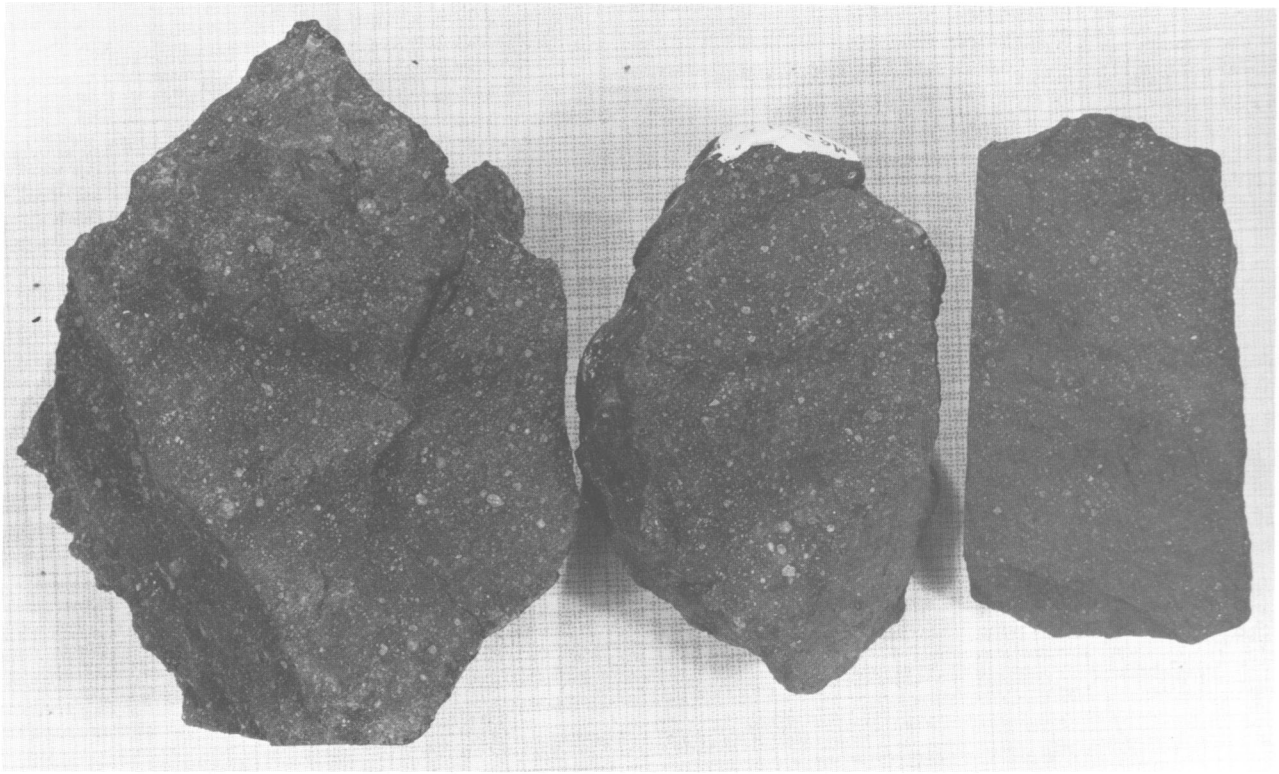

FIGURE 1.—Hand specimens (left to right) of Murchison, Murray, and Mighei C2 meteorites. Murchison and Murray show a closely similar content of inclusions, in contrast to other C2s such as Mighei. The Mighei specimen is 7 cm long.

C2s the matrix is deep black and featureless. Dispersed throughout the matrix are several distinct types of inclusions: (1) *single crystals and crystal fragments* of individual minerals ranging from a few microns up to millimeter size; (2) multi-grained mono- and polymineralic inclusions up to 2mm, which we will call *white inclusions;* (3) *true chondrules* that are spherical or fragmented spherical segments ranging in size from 0.05 to 0.8 mm; and (4) angular xenolithic fragments of another chondrite type that range from a few millimeters up to 13 mm, which we will call *xenolithic fragments.*

In making the distinction between the type 2 and type 3 inclusions above, we have relied upon clear textural characteristics: the *white inclusions* (type 2) have a granular texture—the loosely held mineral grains can be raked out easily with a needle. They are of various shapes and break with the fine-grained black matrix that surrounds them. *True chondrules* (type 3), on the other hand, are relatively hard, well-defined spherical objects—the minerals cannot be scraped out with a needle. They do not break with the matrix but detach as distinct beads. Figure 2 illustrates the difference between the white inclusions and the true chondrules. We emphasize this distinction because casual observers have tended to refer to all the inclusions as chondrules. In certain instances this distinction is not clear-cut.

Of these four types, the first two comprise over 98% of the inclusions seen in the black matrix. Each type will be described after the total mineralogy has been presented.

FIGURE 2.—Chondrule (0.9 mm in diameter) in matrix with white inclusion next to it.

Mineralogy

LAYER-LATTICE SILICATES

The major mineral in Murchison is the black matrix layer-lattice silicate. It comprises 77 vol. % as determined by linear measurements across two hand specimens. Whether this phase is truly black cannot be determined; it may be that the color is due to disseminated submicroscopic amorphous carbon and organic compounds. In addition, finely divided sulfides (such as troilite) are black. Our microprobe results show a consistent matrix carbon content, 1.6–2.2 wt. %, and sulfur, from 1.6–4.1%.

Because the layer-lattice silicate is the major phase in all C2 chondrites, its definite characterization is highly desirable, especially as it has implications for the genesis of this primitive group. In spite of reported attempts by numerous investigators over the past twenty years, definite and consistent results have not been obtained. The only consensus is that it is a hydrated layer-lattice silicate, either of the septechlorite group or serpentine group. Boström and Fredriksson (1966) presented microprobe and X-ray data suggesting it is a ferric chamosite (septechlorite). Bass (1971) has published a thorough review of the literature on this matter.

GENERAL CONSIDERATIONS.—Because the matrix phase comprises the dominant mineral making up Murchison and because the other phases are notably iron-poor, the bulk of the iron oxide in the whole meteorite analysis must be in the matrix phase. Serpentines in general are most often iron-poor and magnesium-rich. In C2 meteorites it has been believed that magnetite, submicroscopically disseminated in a magnesian serpentine, could account for the bulk iron content. In Murchison, however (and probably in other C2 meteorites), magnetite is only a trace mineral (cf., "Spinel Group Minerals"); the weak magnetic properties of the matrix appear to be due to an Fe-S-O phase (cf., "Poorly Characterized Phases").

On the other hand, the low total aluminum content of the meteorite argues against normal septechlorites. The only known (terrestrial) septechlorites with low Al and high Fe are cronstedite and greenalite. These, however, have too low magnesium to account for the bulk Mg content of the

meteorite analysis. Frondel (1962) has reported on the serpentine, ferroantigorite (formerly called jenkinsite), a platy polytype or serpentine. On compositional grounds it might be comparable to the matrix material in Murchison.

COMPOSITIONAL EVIDENCE.—The H_2O content of the matrix can be estimated from that fraction of the water content of the meteorite liberated above 105°C. This fraction is calculated from the amount of hydrogen liberated above this temperature and is not a uniquely determined quantity, for some hydrogen may be released from a small amount of organic matter. In our analysis the total water is 12.1 wt. %; 8.8% is H_2O+ (105°C) (Table 1a) which is in good agreement with the 8.95% reported by Jarosewich (1971) on a drier specimen of Murchison. The matrix constitutes 77 vol. % of the meteorite with the inclusion (mainly low iron olivine and pyroxene) occupying the remaining 23 vol. %. Assuming an average density of 3.3 for the inclusions, the density of the matrix is then 2.71 as deduced from the measured density of 2.85 for the meteorite as a whole. Thus the matrix comprises 73.4 wt. % of the meteorite and contains most of the H_2O+, which amounts to 12.0 wt. % (circumstantially almost equal to the total analyzed H_2O).

TABLE 1a (wt. %).—Comparison of chemical analyses of Murchison meteorite

	This Work	Data of Jarosewich (1971)
Fe^0	0.03	0.13
Cu	0.015	n. d. (6)
NiO	1.73	1.75
CoO	0.076	0.08
FeS	(1)	7.24
SiO_2	27.22	29.07
TiO_2	0.099	0.13
Al_2O_3	2.05	2.15
Cr_2O_3	0.402	0.48
FeO	(1)	22.39
Fe_2O_3	(1)	n.d.
MnO	0.22	0.20
MgO	18.90	19.94
CaO	1.75	1.89
Na_2O	0.57	0.24
K_2O	0.034	0.04
P_2O_5	0.23	0.23
$H_2O(+)$	8.80	8.95
$H_2O(-)$	3.26	1.14
SO_3	2.38	0.90
S	0.49	(4)
S=	1.81(2)	(3)
C	1.91 (Total)	1.85
CO_2	n.d.	1.00
N	0.096	n.d.
	(5)	99.80
Total Fe	20.44	22.13
Total S	3.24_8	3.00

(1) See discussion in section - Wet Chemical Analysis.
(2) A calculated value. Total S -[S as SO_3 + elemental S]
(3) Sulfide sulfur included in FeS value.
(4) No elemental sulfur detected.
(5) No summation since values for FeS, FeO and Fe_2O_3 are not assigned.
(6) n.d. - Not determined.

TABLE 1b (atom %).—Comparison of chemical analyses of Murchison on a volatile (C, H, N, O, S) free basis

	Basis	
	This Work	Calculated from the Data of Jarosewich (1971)
Fe	25.85	26.46
Ni	1.63_6	1.56_4
Co	0.071_3	0.071_5
Si	31.99	32.29
Ti	0.146	0.108
Al	2.82_2	2.81_5
Cr	0.37_4	0.42_2
Mn	0.21_8	0.18_8
Mg	33.12	33.04
Ca	2.20	2.25
Na	1.30	0.51_8
K	0.05_1	0.05_7
P	0.21_4	0.21_6

TABLE 2a.—Electron microprobe analysis of Murchison matrix

	1.	2.	3.	4.
SiO_2	23.4	26.2	23.4	25.9
Al_2O_3	3.1	3.5	3.1	3.4
Cr_2O_3	0.3	0.3	0.3	0.3
Fe_2O_3	-	-	7.6	8.4
FeO	34.1	38.2	27.3	30.3
MgO	15.1	16.9	15.1	16.7
CaO	0.9	1.0	0.9	1.0
MnO	0.2	0.2	0.2	0.2
NiO	1.5	1.7	1.5	1.7
H_2O	-	12.0	-	12.0
Sum	78.6	100.0	79.4	99.9
	Number of ions*			
Si	1.49		1.45	
Al	0.23	1.73	0.22	2.04
Cr	0.01		0.01	
Fe^{+3}	-		0.36	
Fe^{+2}	1.81		1.42	
Mg	1.43		1.39	
Ca	0.06	3.39	0.06	2.96
Mn	0.01		0.01	
Ni	0.08		0.08	
(OH)	4.54		4.49	

1. Average values for 40 spot analyses by J. Nelen, U.S.N.M., NiO is our datum.
2. Oxides in no. 1 recalculated to 88%, H_2O content is calculated from bulk H_2O^+ (see text).
3. 20% of Fe in no. 1 assigned as Fe^{+3}.
4. No. 3 recalculated to 88%, H_2O = 12.0%.

* Calculated to 9(O, OH).

The major element composition of the matrix was obtained from electron microprobe analyses. The average of three analyses kindly supplied by J. Nelen of the National Museum of Natural History are given in Table 2a. The low summation is due to several factors: the major one is the water content; oxides present in amounts less than 0.3% were omitted because of their extreme variability. Our microprobe analyses contain amounts for C and S of 1.7 and 3.3 wt. %, respectively, these elements are probably not a part of the layer-lattice silicate; additional factors involve the porosity of the specimen and the nonideality of the polished surfaces of the fine-grained matrix. The averaged analysis was recalculated to 88 wt. % to allow for the estimated water content of 12 wt. %.

The composition (Table 2a) is adjusted to assign approximately 20% of the analyzed iron as ferric so as to satisfy a tetrahedral to octahedral site ratio of 2/3. The low silica content corresponds more closely to that of a chlorite than to that of a serpentine. The estimated water content may be too high since the calculated oxygen to OH ratio of unity is less than the ideal ratio of 5 to 4. Based on composition alone it does not appear to compare favorably with any known layer-lattice silicate.

X-RAY EVIDENCE. — Approximately twelve X-ray powder patterns (film) were taken of the black matrix from several areas on different specimens of the meteorite. Although sampling was done under the binocular microscope so as to avoid visible contamination, extra lines appeared on some patterns which were not common to others. All patterns, however, contain approximately nine lines in common and these provided a starting point for the identification (Table 3). In some cases the impurity lines could be assigned to either olivine or calcite, but two prominent lines (intensity 3 to 5) at 6.1 Å and 5.4 Å were not positively correlated with each other. Since the 6.1 Å line was generally present on samples selected from unusually black areas of the matrix, it was thought that this might be due to an organic compound. Overnight treatment of these samples with various organic solvents produced no effect on the patterns. But a five minute treatment with 2% nital eliminated the 6.1 A line with no other effects to the overall pattern. Except for the conclusion that the unknown phase was acid soluble, no further attempt was made to

TABLE 2b.—Electron microprobe analyses of "spinach" phase, Murchison meteorite

	This Work		U.S.N.M.	
	1.	2.	3.	4.
SiO_2	28.0	28.0	23.4	23.4
Al_2O_3	2.6	2.6	3.7	3.7
Cr_2O_3	0.4	0.4	0.2	0.2
Fe_2O_3	-	2.3	-	2.0
FeO	29.3	27.3	36.8	35.0
MgO	19.9	19.9	11.6	11.6
CaO	-	-	0.3	0.3
MnO	-	-	0.1	0.1
Sum	80.2	80.5	76.1	76.3
	Number of ions*			
Si	1.70	1.68	1.61	1.59
Al	0.19	0.19	0.30	0.29
Cr	0.02	0.02	0.01	0.01
Fe^{+3}	-	0.10	-	0.11
	1.91	1.99	1.92	2.00
Fe^{+2}	1.49	1.37	2.11	1.99
Mg	1.80	1.79	1.19	1.18
Ca	-	-	0.02	0.02
Mn	-	-	-	-
	3.29	3.16	3.32	3.19
(OH)	4.00	4.00	4.00	4.00

1. Associated with Fo 99 in chondrule, E. Olsen analyst.
2. Recalculated, assuming 7% Fe as Fe^{+3}
3. Composition of associated olivine not determined. J. Nelen, analyst.
4. Recalculated, assuming 5% Fe as Fe^{+3}

* (OH) set to 4.00, formula calculated on the basis of 7 oxygen equivalents.

TABLE 3.—X-ray powder patterns* of the matrix material from the Murchison, Murray, and Mighei meteorites

Murchison		Murray		Mighei		Assignments
d(Å)	I	d(Å)	I	d(Å)	I	
7.2	10	7.1	10	7.2	10	C
-	-	6.0	1	6.0	5	A.S.
5.4	1	5.4	1	5.4	1	U
4.7 Broad		4.7 Broad		4.7	1	C
4.3 Band		4.3 Band		4.51	2	A.S.
3.9	1	3.9	1	-	-	C
3.62	1	3.62	1	-	-	?
3.58	5	3.58	8	3.57	8	C
-	-	-	-	3.43	FT	?
-	-	-	-	3.33	FT	?
-	-	2.88	1	2.86	1	?
-	-	-	-	2.77	1	A.S.
2.70	2	2.70	3	2.69	2-	CM+CH
-	-	-	-	2.61	1	A.S.
2.53	8	2.54	6	2.53	10	CH
2.43	3	2.43	4	2.44	1	CM
2.30	1	2.29	1	2.36	1	C
2.16	4	2.16	3	2.16	6	CH
2.03	1	2.03	1+	2.03	1	CM
1.79	2	1.785	2	1.785	4	CH
-	-	1.68	2B	1.67	1B	C
1.57	3	1.575	3	1.57	3	C
1.54	3	1.540	2+	1.535	3	C
1.49	1	1.49	1	1.49	2	CH
1.44	1	1.44	1	1.438	1	C

*Fe radiation, Mn-filter, 114 mm Philips powder camera. Intensities are visual.
Abbreviations: B = broad; CM = monoclinic chamosite, CH = Hexagonal chamosite, C = lines common to CH and CM; A.S. = acid soluble. U = unidentified fibrous phase.

identify it. Samples showing a 5.4 Å spacing were mounted and polished. These were found to contain several percent of two phases, which displayed massive amorphous and fibrous textures, respectively. They are ubiquitous in all sections of Murchison studied (cf. "Poorly Characterized Phases"). The fibrous phase is characterized by a strong 5.4 Å reflection.

Based on the nine lines common to all patterns of the matrix material certain similarities exist with the septechlorite, chamosite, and the serpentine (ferroantigorite).

Carroll (1970) noted that a trio of medium intensity X-ray peaks at 2.67, 2.40, and 2.15 Å are diagnostic for chamosites. Our matrix material patterns show this trio at 2.70, 2.44, and 2.16 (the small shifts in d-spacings due to compositional differences). This, in itself, could be compelling evidence to establish this material as chamosite. Our X-ray pattern of ferroantigorite from O'Neil Mine, Orange Co., New York (Field Museum sample M3641), however, shows the same three lines present, 2.72, 2.43, 2.17 Å. These, however, are not uniformly of medium intensity, rather the 2.72 line is exceedingly weak. Because our 2.70 line is stronger, and the trio approximates the intensity pattern of chamosite, we regard a chamosite designation of the matrix material as a slightly better possibility than ferroantigorite (or any other serpentine-group mineral). Boström and Fredriksson (1966) have concluded that the matrix material in the Cl meteorite, Orgueil, is a ferric chamosite primarily on compositional grounds.

For comparative purposes X-ray powder patterns were obtained on the matrix material of Murray and Mighei, and these are presented in Table 3 together with that of Murchison.* Aside from a few impurity lines the d-spacings of corresponding lines on the three patterns are in agreement, but significant differences exist in the relative intensities of some lines, especially those that correspond to the prominent lines of either monoclinic or hexagonal chamosite. The intensities of the line at 2.43 Å—monoclinic—vary inversely as those at 2.53 and 2.16—both hexagonal—(for a comparison of both forms of chamosite, see Brindley, 1951 or ASTM card 7–315). It can be seen that the ratio of hexagonal to monoclinic chamosite is greatest for Mighei, intermediate for Murchison, and least for Murray. Although this relationship may not be representative of the matrix material in these three meteorites, the fact that a mixing ratio exists for the samples X-rayed supports the preference of chamosite rather than a serpentine mineral as the predominant mineral in the matrix material. When present, the line at 6.1 Å is removed from all samples when treated with 2% nital for five minutes, in the case of Mighei, lines at 4.51, 2.77, and 2.61 are also eliminated by this treatment. It should be noted that our pattern of Mighei shows a number of differences when compared to the pattern published as "Murray F" by DuFresne and Anders (1962) which they obtained from Mighei. Their pattern contains 9 extra lines that can be assigned to the strongest lines of olivine. Aside from the olivine impurity, the remainder of the pattern is in good agreement with ours.

As a further check on the properties of the matrix material a series of heating experiments were undertaken. A sample of Murchison matrix was

* Samples invariably contained impurities, as evidenced by the spotty character of some lines; it was found that nonrotation of samples during exposure simplified the distinction between the fine-grained matrix and coarser grained impurities.

TABLE 4.—X-ray powder patterns* of Murchison matrix material in an evacuated silica capillary following each stepwise heating period.

Not Heated		3.7 Days 245°C		7.7 Days 245°C		1.7 Days 340°C		5.8 Days 340°C		24 Days 340°C		12 Days 400°C		19 Days 450°C		33 Days 450°C		Phase
d(Å)	I	d(Å)	I	d(Å)	I	d(Å)	I	d(Å)	I	d(Å)	I	d(Å)	I	d(Å)	I	d(Å)	I	
7.2	10	7.1	10	7.1	10	7.1	10	7.1	10	7.1	8	7.1	8	7.4	2	-	-	C
5.4	3	5.4	1															(1)
				3.9	1			3.9	FT									C
3.58	7	3.58	8	3.58	7	3.58	7	3.58	7	3.58	6	3.58	3	3.60	FT	-	-	C
				3.33	FT							3.50	2	3.50	2	3.50	FT	?
				2.97	1	2.97	2	2.97	3	2.97	3	2.97	3	2.97	4	2.96	4	M
				2.85	1													?
2.70	2	2.70	1	2.70	2	2.70	1	2.70	FT	2.70	FT	-	-	-	-	-	-	CM+CH
								2.62	FT	2.64	1	2.65	2	2.65	3	2.65	2	FeS
2.54	7	2.54	8	2.54	8	2.54	8	2.54	9	2.54	8	2.53	10	2.52	10	2.52	10	(2)
2.44	1	2.44	1	2.44	1	2.44	2	2.45	1	2.44	1	-	-	-	-	-	-	CM
2.17	2	2.17	2	2.16	2	2.16	2	2.17	2	2.16	2	2.16	2	-	-	-	-	CH
2.12	1													2.09	2	2.09	2	M
				2.04	1	2.05	2	2.05	2	2.05	3	2.06	3	2.06	3	2.06	2	FeS
1.79	FT	1.79	FT	1.79	FT	1.79	1	1.79	1	1.79	1	1.79	1	-	-	-	-	CH
						1.72	1	1.72	2	1.72	2	1.72	1	1.72	1	1.72	1	M
						1.61	FT	1.61	FT	1.61	1	1.61	2	1.62	4	1.61	3	M
1.57	3	1.57	3	1.57	2	1.57	2	1.57	2	1.57	2	1.57	2	-	-	-	-	C
1.54	2	1.54	2	1.54	1	1.54	1	1.54	1	1.53	1	1.53	FT	-	-	-	-	C
				1.48	1	1.48	1	1.48	FT	1.48	1	1.48	2	1.48	5	1.48	4	M
								1.31	FT	1.32	FT	-	-	1.32	1	1.32	1	FeS+M
																1.092	3	M
																1.048	2	M
																0.856	1	Mx_1
																0.854	1	Mx_2

*Cu radiation, Ni-filter, 114 mm Philips powder camera. Intensities are visual.
Abbreviations: FT = faint trace; CM = monoclinic chamosite; CH = hexagonal chamosite; C = lines common to CM and CH; A.S. = unidentified acid-soluble phase; (1) = unidentified fibrous phase; (2) = line common to M and CH; M = Magnetite.

sealed in vacuo in a silica capillary with a minimum of empty space and heated for various times at increasing temperatures. After each heating period the capillary was air quenched to room temperature and X-rayed. The results are shown in Table 4. The major effect is the decomposition of the layer-lattice structure, which begins at 340°C and is practically complete after the final heating period at 450°C. Magnetite, not present in the unheated material, begins to form about 100°C lower than the apparent decomposition temperature of the silicate and becomes the major phase at 450°C. A significant side effect involves the decomposition of the unidentified fibrous phase (with the characteristic 5.4 Å line) at 245°C to form a new phase, which is most probably troilite (lines at 2.65, 2.06, and 1.32 Å). Of minor importance is the occasional appearance of weak lines as noted in the footnote to Table 4. These may be due to local impurities present along the length of the capillary.

A sample of ferroantigorite from the O'Neil Mine, Orange County, New York, sealed in an evacuated silica capillary and heated at 450°C for 50 days showed that some alteration occurred to form fayalite, but that ferroantigorite persisted as the major phase. These differences observed for the thermal stability of matrix Murchison material and ferroantigorite support the X-ray results that they are not identical. Unfortunately a clean specimen of chamosite was not available on which to perform similar experiments.

Aside from all of these considerations there are problems attending the use of terrestrial minerals of the septechlorite and serpentine groups as reference materials. Often many polymorphic forms exist in a single terrestrial occurrence of a mineral that may be characterized by one published powder pattern. An example in point is the reported existence of eight polymorphs of cronstedite by Steadman and Nuttall (1963) for the type-locality in Cornwall. A powder pattern for this mineral as presented on ASTM card 17–470 could contain contributing reflections from several polymorphs. Since these polymorphs were discovered on single crystal photographs there is usually no assurance that each has the same composition as the bulk material. The relative amounts of these phases of uncertain compositions may vary sufficiently in a meteoritic environment to mask or obliterate a strict comparison with terrestrial counterparts.

Ultimately there may be little justification for discussion of the nature of *the* matrix material for carbonaceous chondrites; there may be several minerals and/or coexisting polymorphs of several minerals of various compositions. Kerridge (1969), using selected area electron diffraction techniques, has found a wide range of unit cell parameters for meteoritic layer-lattice silicates, which suggested to him corresponding variability in compositions.

A polished matrix specimen was treated with warm concentrated phosphoric acid for 30 minutes. A microscopic gridlike pattern of matrix material was removed leaving "islands" of matrix standing in relief. About half of the matrix was dissolved.

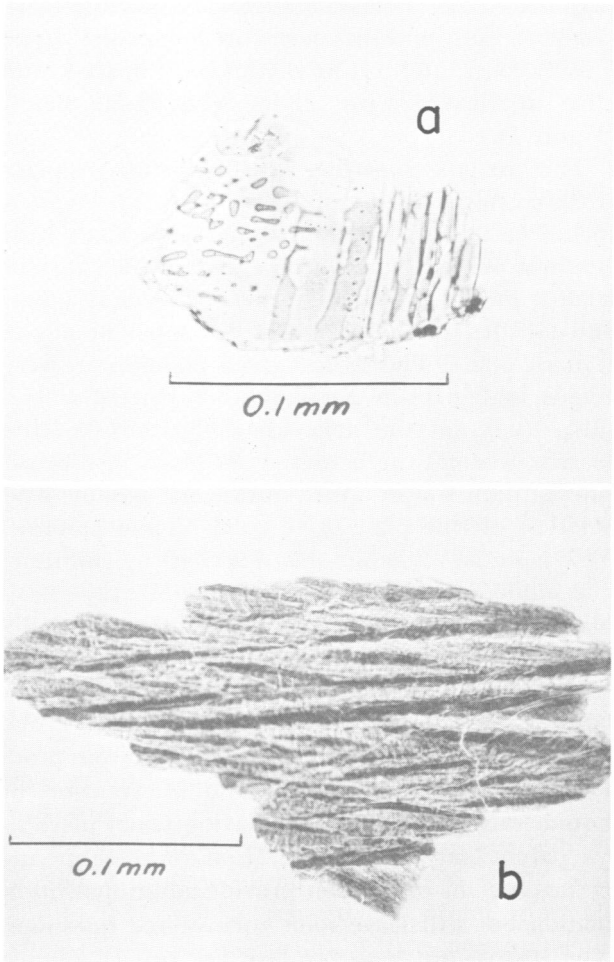

FIGURE 3.—*a*, Plate of olivine (Fo_{100}), parallel to (100), containing oriented glass stringers and blebs; *b*, plate of green hydrated silicate called the "spinach phase" in text. Alternations of *a* and *b* impart a micaceous appearance to this type of inclusion.

This suggests that the matrix consists of at least two phases.

OTHER LAYER-LATTICE SILICATE.—Outside of the matrix, within some inclusions, we found a separate and unique occurrence of a layer-lattice silicate. This silicate may or may not be the same, mineralogically, as the matrix material, for its appearance and mode of occurrence set it apart from the matrix material; the two may not be related genetically. This silicate is characteristically a transparent spinach-green color and to distinguish it in our discussion we will call it the "spinach" phase.

It is found in four distinctive settings: (1) interstitially between, and coating, forsterite (Fo 99) grains; (2) as complete inclusions of "spinach" within the black matrix; (3) interstitial to forsterite (Fo 99) grains within some true chondrules (type 3 inclusions); and (4) as rhythmically spaced lamellae interleaved with olivine (Fo 99–50 plates) (Figure 3).

The last type of setting with its distinctive platy texture can almost be considered a separate type of inclusion. Plates of unaltered olivine alternate with isotropic or weakly anisotropic plates which vary in color from light to dark green. The color is apparently related to the degree of development of the spinach phase. The darker green platelets are very fragile and give an X-ray powder pattern resembling (but not the same as) the patterns of the matrix; whereas the lighter green plates give broad lines of both a layer-lattice silicate and olivine. The colorless olivine plates give good olivine patterns. This material resembles that described by DuFresne and Anders (1962) for Mighei and Murray: ". . . olivine has been divided by the penetrating material into a series of thin parallel plates with rather a micaeous appearance, although diffraction shows nothing present but olivine and Murray F." The authors consider Murray F to be an alteration product of olivine produced by the intervention of liquid water, "the alteration having taken place in the parent body." Our observations on these specific occurrences in Murchison provide additional information but still leave some unanswered questions. The texture of these "lit par lit" spinach-olivine inclusions ends abruptly at the surrounding matrix. In section there are no obvious adits leading to the inclusion; additionally, nearby olivine crystals or fragments within the matrix may be unaltered, suggesting that the alteration is pre-Murchison in origin.

The plates of olivine are always parallel to the (100) plane, as evidenced by a centered acute bisectrix interference figure, and they contain numerous glassy inclusions of various shapes from distorted spheres to elongated blebs or ribbons (Figure 3). Glassy blebs within some of the plates of olivine are oriented in directions parallel to or 45° to the extinction directions and thus occur along crystallographic directions. We have not analyzed these glasses as most are only a few microns wide in their shortest direction. Lacking compositions, we can say nothing about their origin or why they are so numerous. Their abundance, however, suggests that they are somehow related to the degree of olivine alteration. It is possible that the spinach formed by the replacement of olivine plates which were loaded with nonresistant glass. The surviving unaltered olivine either contained discrete glass blebs protected by olivine, or perhaps the unaltered glass was simply more resistant.

One clue that possibly illustrates the initial development of the spinach phase comes from a chondrule in a thin section of Murray. Parallel bands of olivine are interleaved with alternating bands of light-green mottled isotropic glass. The green is confined to the glass; bands of olivine are unaltered.

The quality of the X-ray patterns for the matrix material did not permit comparison of subtleties that would allow more definitive interpretation. Only 9 X-ray lines were obtainable in that case. On the other hand, X-ray patterns of the green spinach phase yield 14 relatively sharp lines that can be assigned to a mixture of monoclinic and hexagonal polymorphs of chamosite; a few weak unidentified impurity lines are usually present.

In the case of the fourth setting, it was noted that the plates of layer-lattice silicate visibly contained impurity phases. An X-ray pattern consisted of 21 lines and was more difficult to interpret. It appeared to consist of a mixture of chamosite, serpentine, and other unidentified phases.

The composition of this spinach phase from a true chondrule is presented in Table 2b, which includes an analysis of the same phase obtained by J. Nelen from an undetermined site in one Murchison section. It is apparent that this phase varies

in composition. Although sufficient data are lacking, this variation apparently has no relation to the composition of the associated olivine; in our occurrence (29.3 wt. % FeO) the associated olivine is practically Fe-free. Both analyses can be calculated to 7 oxygen equivalents as no estimates of H_2O contents can be made. Compared with the matrix material (Table 2a), smaller amounts of Fe^{+3} are required to fill the tetrahedral sites, but clearly there are too many octahedral ions in both spinach analyses. This indicates that nonlayer-lattice silicate impurities are present. They are either amorphous or, if crystalline, are present at levels not permitting X-ray identification. These uncertainties nullify the possibility that the spinach phase is a simple in situ alteration product of olivine.

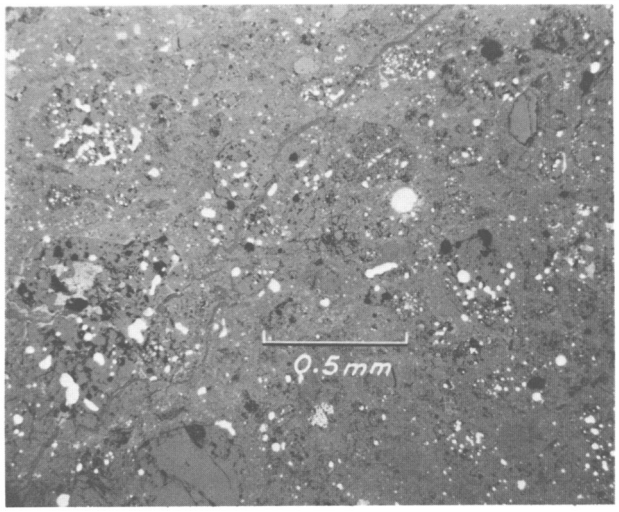

FIGURE 4.—Polished section of an exceptionally metal-rich area. Some troilite is present, but it is less than one percent.

OLIVINE

Olivine is the next most abundant phase, occurring in all four types of inclusions. It ranges in composition—from grain to grain—from Fa 0 to Fa 85, both as internally homogeneous crystals and as strongly zoned crystals. Olivine will be discussed in detail under "Textural Features" and "Mineralogical-Compositional Relationships."

CA-POOR PYROXENE

Both the orthorhombic and monoclinic forms of the enstatite-bronzite series occur, compositions ranging from Fs 1 to Fs 50. No zoning was observed. Many of the orthorhombic crystals gave X-ray patterns of a disordered form (Pollack and Ruble, 1964) with considerable line broadening. Some, however, showed normal ordered patterns. Pyroxene will be treated in more detail later.

CALCIC-PYROXENE

Fragments of calcic-pyroxene occur within the matrix, but are exceedingly rare. Partial analyses performed on some grains gave Fe/(Fe+Mg) ratios of 0.06 to 0.09. Diopside has been found surrounding hibonite in minute white inclusions (cf., "Hibonite" and "Perovskite"). In one instance a dark green augite grain was found.

METAL

Metal is not abundant. In the bulk analysis (Table 1a) it amounts to only 0.03%. A few sections, however, contain abnormally high amounts (Figure 4). It is found mainly within some olivine grains, both in white inclusions and in true chondrules. Some rare isolated grains occur in the black matrix or within Ca-poor pyroxene. Metal grains range in size from submicron blebs up to 0.42 mm in sections we studied. The very few large grains were found isolated in the matrix and not in olivine or pyroxene. The grains are smooth ovate to spherical in shape, which is distinctly different from the angular shapes commonly found in the ordinary chondrites.

A group of metal analyses are given in Table 5. These analyses are of metal grains within olivine (both from white inclusions and true chondrules) and isolated in the matrix. There are no systematic chemical differences between the metals from these three sites.

The outstanding features are the unusually high Cr and P contents, from 0.20 to 0.96 wt. % and 0.28 to 0.37 wt. %, respectively. Metal from all other classes of meteorites, where measurements are available, carry only trace amounts of Cr (less than 0.001%). Indeed, in most instances it is not reported because it is presumably at low trace levels only. Some of the metal in lunar lavas runs up to 0.42% Cr (Taylor, Kullerud, and Bryan,

TABLE 5.—Electron microprobe analyses of metal grains in Murchison

Location of grain			Fe	Ni	Co	Cr	P	Sum
Four grains	1	Center	93.8	5.6	0.40	0.96	0.28	101.0
		Edge	"	"	"	0.85	"	100.9
within	2		94.6	4.3	0.32	0.79	0.32	100.3
single	3		94.0	4.0	0.32	0.80	0.32	99.4
chondrule	4		93.7	4.9	0.35	0.86	0.37	100.2
Two grains								
within	1		90.8	7.4	0.41	0.69	0.29	99.6
single	2		92.2	5.6	0.74	0.78	0.37	99.7
chondrule								
Six grains	1		92.1	5.5	0.40	0.83	0.35	99.2
in	2		93.5	5.0	0.35	0.64	0.37	99.9
black matrix	3		94.0	4.8	0.38	0.73	0.32	100.2
	4		93.6	4.8	0.35	0.49	0.36	99.6
	5		93.7	4.8	0.32	0.77	0.35	99.9
	6	Edge	93.1	6.3	0.42	0.20	0.31	100.3
		to Edge	92.0	7.0	0.43	0.55	0.32	100.3

1971), which is still a factor of 1.7 less than the average Murchison metal (0.7%). Only two grains were large enough to test for Cr homogenity. Scanning across a large (0.42 mm) grain (isolated in the matrix) showed a steady Cr profile of about 0.2% for about half the grain, then rising smoothly to 0.55% at the opposite edge. In the other case, a grain of metal within forsterite in a true chondrule showed a central core of 0.96% Cr falling to 0.85% at the edges.

The average P content of these metal grains is 0.33%. The large 0.42 mm matrix grain was scanned for phosphorus homogeneity. The grain ran generally around 0.32% with a few spots showing up to 0.60%. These spots may be due to small specks of phosphide, although none were visible. No such spot was wide enough for microprobe analysis.

Because of the unusual chemistry of the Murchison metal careful wavelength scans were performed, especially for Si, Ti, V, Mn, Cu, Mo, W, and Pt. None of these was present above detection limits (about 0.05%) although one grain showed a possible Pt content of about 0.07%.

We assume the metal is kamacite; however, we do not have any data that totally rule out other structural states. The grains analyzed were generally too small to scan for homogeneity. The one large (0.42 mm) grain was relatively homogeneous in Ni content, showing a slight rise from 6.3% to 7.0% going across the grain; however, a few isolated spots within it showed lows of 4.7%. Etching of larger grains revealed no observable structural features, plessite areas, Neumann bands, etc.

The recent study of the Fe-Ni-P system by Goldstein and Doan (1972) shows that kamacite with up to 0.4% P and up to 7% Ni can exist without schreibersite being formed down to a temperature of 550°C. These are the upper limits of P and Ni values in the Murchison metal. Grains of kamacite with as little as 0.3% P and 4% Ni could represent even lower temperatures (450–500°) without the formation of schreibersite. The effect of up to 0.9% Cr on this is unknown.

The unusual content of Cr in the Murchison metal will be discussed under "Chromium and Phosphorus in Metal." We also note that a complete chondrule made of metal, with some schreibersite, was found in one single instance. It is described under "Phosphorus Minerals."

SULFIDES

Both troilite and pentlandite were found, the former several times more abundant than the latter. The predominance of troilite over pentlandite in the case of Murchison disagrees with the reverse relation in other C2s (Ramdohr in Mason, 1962-63). The troilite commonly shows a mottled appearance due to finely disseminated pentlandite (Figure 5). The mottling ranges from submicron

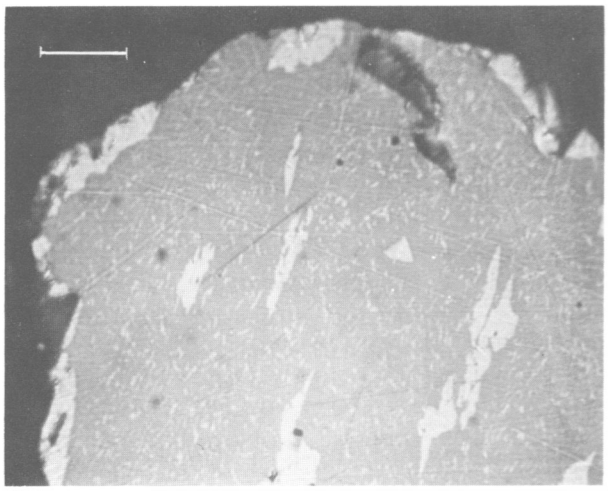

FIGURE 5.—Pentlandite (light) within troilite matrix. Oil immersion, scale bar is 10 microns.

size up to 5-micron patches of pentlandite. The nickel content of the troilite ran as low as 0.2 wt. % where the mottling was absent entirely, up to 1.7% where the mottling was very apparent. It would appear that the nickel content of the troilite is quite low, comparable to values in other common meteorite types, and that values above 0.2% are due to the minute admixture of pentlandite. Separate analyses of the larger pentlandite grains give Ni=24.4%.

Texturally most of the troilite occurs as angular grains in the matrix; it has a distinct fragmental appearance and is not associated with metal grains. This is in marked contrast to some C3 chondrites, where troilite commonly rims metal grains. Point counting of troilite and pentlandite grains gives an abundance of 0.13 wt. % which is considerably less than the amount that is computed from the bulk chemical analysis, 7.24 wt. % (Jarosewich, 1971). This disparity is because the bulk of the sulfur is not present as troilite but must be finely divided and dispersed in the black matrix. As such it is not visible in an interior section, but its presence is revealed within a band 0.3–0.6 mm wide adjacent to the fusion crust. Atmospheric heating has formed profuse amounts of a light-yellow phase, softer and less reflecting than troilite, which resulted from a reaction between matrix sulfur and iron in unknown states. This soft-yellow phase may be related in composition to the poorly characterized sulfur-bearing phase (see "Poorly Characterized Phases) where it is not associated with the fusion crust, but the two phases differ markedly in mode of origin.

Phosphorus Minerals

No phosphates were seen; however, the phosphide schreibersite occurs as blebs in the chondrule of metal noted earlier, and as rare specks within metal grains in the black matrix. It was never observed in metal grains contained within olivine crystals or contained in true chondrules. This is the first time schreibersite has been reported from any carbonaceous meterorite.

Calcite

Calcite grains were ubiquitous in all sections studied. It occurs principally in the black matrix; however, X-ray patterns of *some* white inclusions showed it to be present there in small amounts. Grains range from a few microns up to 80 microns. X-ray, optical, and microprobe work show it to be free of any cations other than calcium. The grains are frequently polysynthetically twinned.

Whewellite

Whewellite, the calcium oxalate monohydrate, $Ca(C_2O_4).H_2O$, was found in one white inclusion between olivine grains. The X-ray pattern matches the ASTM reference pattern perfectly with no extraneous lines present. Over ten lines were observed. The occurrence in Murchison is logical considering the relatively high organic and calcite content of the meteorite. Terrestrially whewellite is found in organic-rich sediments, plant cells, some kidney stones, and occasionally in hydrothermal deposits.

At 230°C whewellite decomposes to the anhydrous salt (Freeman and Carroll, 1958). This temperature, however, cannot be used as a maximum temperature indicator here because the anhydrous salt is hygroscopic (Miller, 1953). At lower temperatures it would revert to the monohydrate in the water-rich environment within the meteorite. At best a maximum of 480°C may be indicated where the anhydrous salt decomposes to form $CaCO_3+CO$ (Freeman and Carroll, 1958).

Spinel Group Minerals

Three minerals of this group are found in Murchison: spinel proper is found as inclusions within olivine and in white inclusions; chromite is found in white inclusions and as fragments in the black matrix; spherules of magnetite are found in the matrix and occasionally within troilite. The NiO content of the magnetite within the troilite is 0.8%, whereas no nickel is found in the matrix magnetite spherules.

Spinel proper varies considerably in composition, color, and cell size from grain to grain, from pure $MgAl_2O_4$ to compositions with considerable Fe and Cr (Table 6).

All these members of the spinel group occur in trace amounts only. Chromite is somewhat more abundant than the others. Magnetite is quite variable in quantity from section to section, al-

TABLE 6.—Electron microprobe analyses of spinels

	1	2	3	4	5	6
Al_2O_3	71.1	46.5	59.9	67.4	67.3	69.6
Cr_2O_3	0.7	25.4	12.8	2.6	2.1	0.7
TiO_2	0.3	0.3	0.3	0.2	0.2	0.2
FeO	0.1	10.9	2.5	0.6	0.6	0.5
MgO	28.8	18.3	25.7	27.5	28.1	28.3
CaO	n.d.	n.d.	n.d.	1.6	0.1	0.0
Sum	101.0	101.4	101.2	99.9	98.4	99.3
n	1.722	1.855	1.780	n.d.	n.d.	n.d.
a(Å)	8.091	8.182	8.135	n.d.	n.d.	n.d.
	Numbers of ions on the basis of 32(O)					
Al	15.78	11.75	13.95	15.34	15.46	15.73
Cr	0.10	4.30	1.99	0.39	0.33	0.12
Ti	0.05	0.05	0.05	0.03	0.04	0.03
Fe^{+2}	0.01	1.96	0.42	0.09	0.09	0.08
Mg	8.08	5.85	7.57	7.91	8.16	8.09
Ca	-	-	-	0.34	0.02	0.0
$R^{+3}+R^{+4}$	15.93	16.10	15.99	15.76	15.83	15.88
R^{+2}	8.09	7.81	7.99	8.34	8.27	8.17

Notes to Table 6.

Nos. 1,2, and 3 are 50-120 μm grains from 3 different olivine-spinel white inclusions.

Compositions of associated olivines are: Fa_0(No. 1), Fa_{10} (No. 2), Fa_{2-7} (No. 3).

Nos. 4 and 5 are 6 μm grains inside of glass inclusion 1a and 1b resp. Table 8.

Composition of host olivine is $Fa_{0.6}$.

No. 6 is a 12 μm inclusion in $Fa_{0.3}$.

n.d. = not determined

Mn, Zr, K, Na are below background.

though generally lower than chromite. The general low abundance of magnetite runs counter to many statements in the literature that it is a significant phase in all carbonaceous chondrites. Small chips of Murchison are noticeably magnetic. The magnetism, however, may be due to a relatively abundant phase which we have been able only to poorly characterize as a possible Fe-S-O phase (see "Poorly Characterized Phases").

The chromite varies moderately in composition from grain to grain (Table 7). The compositions are notably different from chromites in all other meterorite types (Bunch, Keil, and Snetsinger, 1967; Snetsinger, Keil, and Bunch, 1967; Bunch, Keil, and Olsen, 1970; Bunch and Keil, 1971). The analyses reported in Table 7 are for individual angular fragments dispersed within the matrix in one probe section. These chromites are generally characterized by their Al_2O_3 contents (av. = 14.8 wt. %) and in this respect they are markedly different from those in the ordinary chondrites (av. about 6%), and resemble those from terrestrial igneous rocks (av. about 16%). Of all the meteoritic chromites analyzed in the four references cited, exclusive of those in the brecciated mesosiderites, only a few have Al_2O_3 contents approaching those in Murchison, and they occur in a few members from highly fractionated classes such as the hypersthene achondrites and some irons. If the C2s contain primitive matter, it is surprising that the compositions of the Murchison chromites are so different from those in the abundant chondrites. It is difficult to imagine some process whereby these compositions might be brought to the compositions of ordinary chondritic chromites, especially at temperatures around 800°C where most chondrites are thought to have equilibrated. Only small differences in the compositions of chromites exist between the various metamorphic grades of chondrites, hence metamorphism has only a minor effect in altering chromite compositions. The compositional differences between Murchison and ordinary chondritic chromites were consequently established in some primary process. We can only speculate that the temperatures involved were rather high and close to those in the magmatic range that effected the fractionation of some meteorites with

TABLE 7.—Electron microprobe analyses of chromites

	1	2	3	4	5	6	7	8	9
Cr_2O_3	47.4	46.8	47.1	60.2	48.9	51.4	41.9	50.3	49.2
Al_2O_3	17.3	17.7	18.5	3.2	15.7	10.7	22.3	14.0	14.2
V_2O_3	0.6	0.5	0.4	0.6	0.8	0.7	0.6	0.7	0.7
TiO_2	0.9	0.7	0.6	0.5	1.6	1.7	0.9	1.2	1.4
FeO	26.7	28.4	25.4	32.9	27.4	29.3	27.7	27.2	28.2
MgO	6.2	5.7	8.1	1.3	5.7	4.5	6.9	6.7	5.8
MnO	0.3	0.2	0.2	0.3	0.3	0.3	0.2	0.3	0.3
Sum	99.4	100.0	100.3	99.0	99.4	98.6	100.5	100.4	99.8
	Numbers of ions on the basis of 32(O)								
Cr	9.93	9.80	9.65	14.07	10.25	11.33	8.49	10.60	10.47
Al	5.40	5.52	5.65	1.12	4.90	3.52	6.73	4.40	4.51
V	0.13	0.11	0.08	0.14	0.18	0.15	0.12	0.14	0.15
Ti	0.18	0.14	0.12	0.11	0.32	0.35	0.17	0.24	0.29
Fe^{+2}	5.92	6.28	5.51	8.14	6.07	6.84	5.95	6.07	6.34
Mg	2.45	2.24	3.13	0.57	2.24	1.89	2.63	2.66	2.33
Mn	0.06	0.05	0.05	0.07	0.06	0.07	0.05	0.06	0.06
$R^{+3}+R^{+4}$	15.64	15.57	15.50	15.44	15.65	15.35	15.51	15.38	15.42
R^{+2}	8.43	8.57	8.69	8.78	8.37	8.80	8.63	8.79	8.73
Sum	24.07	24.14	24.19	24.22	24.02	24.15	24.14	24.17	24.15
	Redistribution of ions to allow for an assigned percentage of total Fe as Fe^{+++}								
$\%Fe^{+++}$	8.0	8.0	11.0	9.0	8.0	10.0	10.0	11.0	11.0
$R^{+3}+R^{+4}$	15.99	15.95	15.96	15.98	16.01	15.87	15.97	15.91	15.93
R^{+2}	7.89	8.01	8.01	7.95	7.83	8.02	7.93	8.03	7.94
Sum	23.88	23.96	23.97	23.93	23.84	23.89	23.90	23.94	23.87

Note to Table: The number of divalent ions exceeds the ideal number of 8 and the sum of the quadrivalent and trivalent ions is less than the ideal number of 16. This indicates that either ferrous or ferric ions are in 6-fold coordination. For illustrative purposes, we have recalculated each analysis assuming that from 8 to 11 wt. % of the total Fe may be present as Fe^{+3} but no case is made for its presence. The departure in the total number of cations from 24 may be the result of analytical error.

distinctive compositions such as the irons and hypersthene achondrites. These observations clearly argue against the derivation of ordinary chondrites from C2 chondrites by any process short of melting.

Lawrencite (?)

On many (not all) freshly broken and fusion-crust-covered surfaces we observe scattered, spotty "bleeding" taking place slowly. The bleeding consists of patches, up to several millimeters, of hydrated red iron oxide. In the past such bleeding, especially in irons, has been attributed to the presence of unstable lawrencite. Our attempts failed to definitely identify lawrencite. Whatever unstable phase is causing this, its distribution is not uniform. Individual specimens vary from no spots, to a few scattered spots, to numerous ones. In general, the spots tend to cluster into areas up to a centimeter across.

Hibonite ($CaAl_{12}O_{19}$)

Some very rare white inclusions, 100–150 microns in diameter, have intensely colored blue centers of microcrystalline hibonite needles, the largest 3 x 10 microns. X-ray powder patterns of the blue concentrates were predominantly those of hibonite with minor perovskite. Line spacings and relative intensities of the hibonite pattern were identical to those reported for hibonite from the Leoville meteorite (Keil and Fuchs, 1971). The surrounding white material is spinel and perovskite which may be associated with diopside. One diopside-bearing inclusion was mounted and probed. Diopside forms the outer surface with an intergrowth of diopside, spinel, and perovskite making up the mantle which encloses in turn a core of hibonite. Because of the small width of the hibonite needles, only a partial analysis could be obtained: in wt. %, Al_2O_3 74.5, CaO 8.2, MgO 2.9. It is suspected that several percent of titania may be present analogous to one of the hibonite compositions found in both Leoville and Allende; however, during the course of the analysis epoxy-bubbling obscured the surfaces and forced us to terminate the analysis.

Optically, the needles are strongly pleochroic: ε = colorless, ω = intense blue; refractive indices are 1.78 (ε) and 1.75 (ω); grains from one inclusion had higher indices of 1.80 and 1.77. Hibonite in Murchison marks the first occurrence of this mineral in a C2 meteorite. The blue color and absence of associated gehlenite serves to distinguish this occurrence from those reported in the C3s.

Perovskite

Scattered euhedral crystals of perovskite, $CaTiO_3$ (2 to 4 microns), occur with diopside and spinel which surround patches of hibonite. This is similar to the occurrences in Allende and Leoville in which hibonite is rimmed by perovskite. In those C3 chondrites, however, gehlenite is an accessory mineral. No gehlenite was found in Murchison. Perovskite was identified by its characteristic X-ray powder pattern. A partial probe analysis (uncorrected amounts vs. rutile and grossular standards) gave, in wt. %, 55 TiO_2 and 43 CaO as compared to an ideal composition of 59 TiO_2 and 41 CaO.

Sulfates

Glistening plates (up to 40 microns) of gypsum were found in localized areas on the surfaces of some hand specimens (Figure 6). X-ray patterns were of excellent quality and contained no extra lines. Qualitative microprobe scanning showed no cations other than calcium present above the 2% level. By a series of observations on fresh surfaces

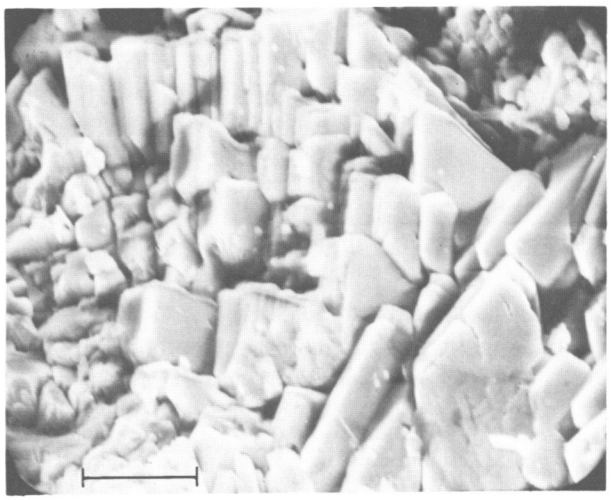

Figure 6.—Scanning electron microscope photograph of gypsum crystals that occur in localized areas on some freshly broken fragments. Scale bar is 20 microns.

it appears that gypsum does occur in Murchison as a preterrestrial phase filling localized short, discontinuous, thin veins. Evaporation on surfaces apparently causes redeposition of intergranular gypsum as large plates. We examined specimens of the C2, Cold Bokkeveld, which have fracture surfaces created by sampling breakage in museum collections over many years. All of these post-terrestrially made surfaces are covered by numerous, outward-projecting plates of gypsum.

No other sulfate phases were found; however, it is possible others may be present. This is inferred from the appreciable amounts of Na and Mg in the water-soluble fraction determined in the bulk chemical analytical results (see "Chemical Analysis Discussion and Comparison").

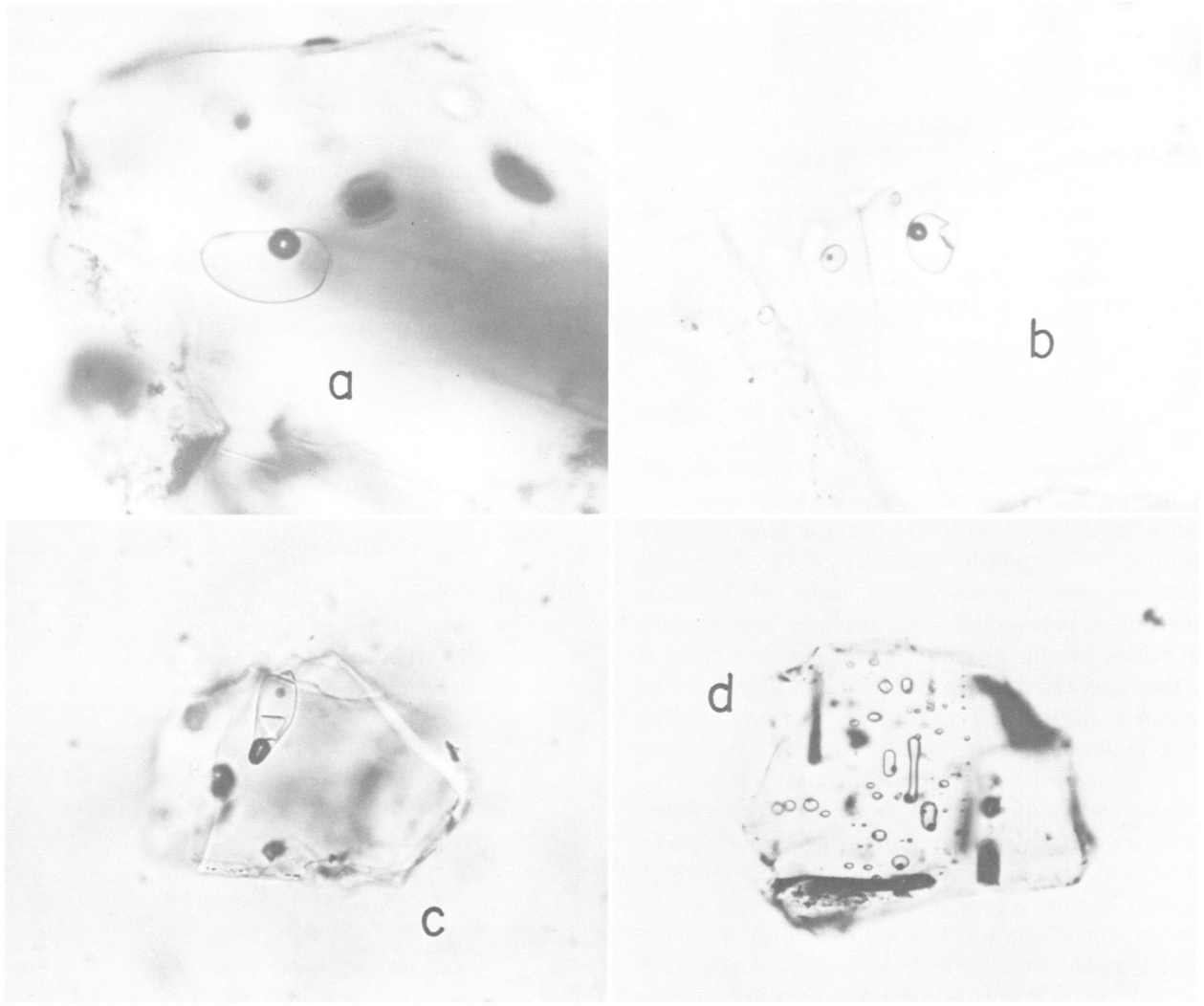

FIGURE 7.—Assorted calcium aluminum silicate glass inclusions within olivine: *a*, largest inclusion found is 36 microns in diameter and contains a void bubble. Smaller inclusions are present but are not in focus; *b*, 18-micron inclusion with void bubble and spinel crystal attached to outside surface of inclusion. Smaller inclusions (not in sharp focus) do not have spinel crystals; *c*, elongated inclusion (11 by 29 microns) containing void bubble and euhedral spinel crystal. *d*, olivine fragment (220 microns in diameter) containing numerous inclusions elongated parallel to extinction directions.

Glasses

Rare shards of glass that yielded no X-ray pattern were observed in some polished sections. In addition, most true chondrules (type 3 inclusions) contain small amounts of glass. The compositions vary moderately and average around 77% SiO_2, 14% Al_2O_3, 9% CaO, and less than 1% of Na_2O + K_2O. Of special interest is the occurrence of ovate glass inclusions (up to 36 microns in diameter) within single olivine crystals that are isolated in the matrix (type 1 inclusions, Figure 7). Olivine grains within the loosely consolidated multigrained aggregates (type 2 inclusions) also contain these inclusions. The latter occurrence has not been studied in detail, so our description and discussion of the inclusions apply only to those within the isolated subhedral to euhedral olivines.

These inclusions are similar in appearance to those noted in the Chainpur chondrite by Dodd (1969) and to the melt inclusions in lunar and terrestrial olivines described by Roedder and Weiblen (1971). An inclusion may or may not contain void bubbles, spherules of metal, an iron sulfide, or euhedral spinel crystals. Interior walls of some void bubbles are lined with an iron sulfide (presumably troilite), suggesting that a sulfur-containing vapor occupied the bubble volume at elevated temperatures. The size of the bubbles varies considerably, and there appears to be no correlation with the size of the inclusion. For twelve inclusions measured, the volume percentage of bubble to inclusion varies from 1 to 14; some inclusions have no bubble. This variation in bubble size cannot easily be accounted for by a simple differential contraction mechanism between inclusion and host during cooling. Alternatively, bubble occupancy by vapors under varying pressures may account for the observed variation. The smooth ovate shapes of the glass inclusions (most are spherical but some are elongated) indicate that they formed from a liquid phase. Aside from the occasional presence of spinel (Table 6), inclusions contain no other nonopaque crystalline phases; the glasses have not devitrified. The persistence of a glass during cooling is in agreement with the observations by Roedder and Weiblen on lunar olivines where, with one exception, inclusions less than 22 microns remained all glass. Our largest glass inclusion is somewhat larger, 36 microns.

Microprobe analyses of these glasses (Table 8) show wide variability in composition, though individually they are of uniform composition. One bleb, however, contained two glass phases exhibiting distinctive reflectivites in the section. Their compositions are given as 4b and 4c in Table 8. Both phases are intergrown. Compositional features common to most of the individual analyses are the high Ca and Al and low alkali contents and thus are very different from the alkali-rich glasses observed in unequilibrated ordinary chondrites (Kurat, 1967; Fuchs, 1968; van Schmus, 1967). Ca and Al rich inclusions are found in C3 chondrites, but consist of several crystalline phases. The enrichment of Ca and Al within small areas in both C2 and C3 meteorites suggests a common source for this material in both types of meteorites, but not necessarily a genetic relation between them.

Since the melt inclusions in Murchison olivines differ in composition, it might appear that they did not originate from a common source; this conclusion, however, may not be valid. The average weight ratio of Ca/Al of all glasses is 1.13, which

TABLE 8.—Electron microprobe analyses of glass inclusions in olivine

Incl. No.	SiO_2	CaO	Al_2O_3	FeO	MgO	MnO	K_2O	Na_2O	TiO_2	Cr_2O_3	Sum
1a	48.2	17.0	27.4	0.2	6.7	0	0	0.01	0.9	0.2	100.6
1b	48.1	21.3	21.6	0.3	3.6	0	0	0.01	1.1	0.1	96.1
2	45.4	21.6	25.7	0.2	4.6	0	0	0.01	0.9	0.2	98.6
3	63.1	10.7	12.9	7.1	2.6	0.1	0	0.3	0.6	0.2	97.6
4a	45.4	22.9	25.2	0.1	3.3	0	0	0	1.0	0.2	98.1
4b	43.6	23.8	21.0	0.2	9.4	0.03	0	0	2.1	0.1	100.2
4c	54.7	17.3	25.0	0.1	1.6	0	0	0.2	0.3	0	99.2
5	44.9	20.4	28.0	0.2	3.8	0	0	0	0.9	0.2	98.4
6	53.1	17.4	23.7	0.2	4.0	0	0	0	0.6	0.3	99.3
7	49.4	21.1	24.1	0.1	3.7	0	0	0.03	0.6	0.1	99.1
8	74.2	9.0	8.7	2.0	2.2	0.1	0.2	1.4	0.4	0.2	98.4
9	57.3	17.4	17.3	0.1	7.5	0.03	0.1	0.5	0.5	0.3	101.0
10	47.7	20.9	24.6	0.2	3.7	0.03	0	0.03	0.8	0.3	98.3
11	53.7	12.8	16.5	6.8	1.7	0.1	0.4	1.8	0.8	0.03	94.6
Av.	52.1	18.1	21.6	1.3	4.2	0.03	0.05	0.3	0.8	0.2	98.7

Notes: (1) 1a and 1b are 2 separated inclusions in one olivine grain; 4a is a homogeneous inclusion which is isolated from the intergrowths of 4b and 4c in the same olivine grain; remainder are single inclusions in different olivine grains.

(2) The fayalite content (in mol. %) of host olivines is 0-1 except for the following: No. 3 (25-45), No. 8 (3-8), No. 11 (23-35).

is not too different from that of 1.09 for all chondrites and basaltic achondrites (Ahrens, 1970). Thus these glasses may be primordial condensates from a gas cloud that supplied all Ca and Al to meteoritic matter. Further implications will be discussed later under "Summary and Discussion of Observations."

It should be pointed out, incidentally, that there is a relationship between the FeO content of a given glass bleb and its host olivine. Glasses containing less than 0.3 wt. % FeO occur in unzoned, iron-poor olivines. The three relatively FeO-rich glasses occur in zoned olivines, the average FeO content of which increases with that in the glass. This correlation probably reflects the FeO environment of the source material and does not result from an in situ diffusion of iron between inclusion and host. Microprobe traverses (1 micron beam diameter) show that no compositional gradients exist between host and inclusion. Abrupt changes in composition are confined to bands 2 microns wide. Zoning in host olivines is not influenced by the presence of inclusions.

Melt inclusions in minerals from igneous rocks may be formed by trapping fluid during fractional crystallization, the composition of a melt inclusion is then in equilibrium with its host at the temperature of the liquidus. Moreover, all inclusions within a single host should have the same composition. With regard to the latter condition, we have data for two such olivines, both of which contain glasses that differ in composition (glasses 1 and 4, Table 8). While it is possible that an olivine crystal growing in a magma could trap melt inclusions of different compositions, we can find no other evidence for a magmatic origin for these olivines.

A few preliminary heating experiments on olivines with unanalyzed inclusions were performed at 100°C intervals from 1200 to 1400°C for periods of several hours followed by air-quenching to room temperature. About six inclusions within each of two crystals were observed microscopically and photographed before and after each heating period. In a few cases, crystals of unknown compositions appeared in glass (which initially was all glass) and then disappeared after heating to higher temperatures. Either solution of some olivine had occurred to change the composition of the inclusion (some inclusions did become larger), or some annealing occurred and was erased at the higher temperature. The lowest liquidus observed was between 1200 and 1300°C as indicated by a shift in bubble position, but bubbles in other glasses in the same olivine did not move even after 1400°C. These observations support the compositional evidence above that different inclusions within an olivine crystal have different compositions. Furthermore, their compositions in some cases would have been altered if they coexisted with their host under these heating conditions.

Phase diagrams can be examined to test for inclusion—host equilibria. The normative composition (wt. %) for the average for all glasses in Table 8 is 60% anorthite, 27% diopside, and 13% silica. But because the compositional range is appreciable, each can be treated separately. For simplicity FeO is added to MgO. The major component oxides then lie within the quaternary system CaO-Al_2O_3-MgO-SiO_2. The diagrams at one atmosphere of Prince (1954) and Morey (1964) are applicable for a few compositions, but for most compositions the diagrams of Osborn et al. (1954) are more appropriate as they present planes in the tetrahedron for constant alumina contents in increments of 5% in the range from 5 to 35%. The major conclusion deduced from these glass compositions is that they are not in equilibrium with olivine at liquidus temperatures and therefore cannot represent compositions of melts from which olivine crystallized. There is no olivine primary phase field in planes with constant alumina equal to or greater than 25%. Eight of the glasses lie close to or within these planes. Three glasses (1b, 4b, 9) lie within the anorthite field; cristobalite or tridymite are primary crystallates for glasses 3 and 8, and number 11 has too low a summation for consideration.

Two melt inclusions (1a and 1b) contain euhedral spinel crystals. The question arises whether spinel crystallized in situ from a melt higher in MgO and Al_2O_3 than the present melt compositions. If this be true, then the initial composition of 1a (for example), adjusted to include the amount of observed spinel (33 wt. percent), becomes in wt. percent: SiO_2 32.1, CaO 11.8, Al_2O_3 40.7, FeO 0.4, MgO 13.7, TiO_2 0.7, and Cr_2O_3 1.1. This composition has not been observed for any spinel-free inclusion. Furthermore, euhedral spinels (Fe- and Cr-free) are found within olivine not associated with a melt inclusion. This suggests that

euhedral spinel predated formation of melt inclusions and olivine. Early-formed spinel could have nucleated later condensates.

As was mentioned earlier, in appearance these glassy inclusions resemble the melt inclusions found in olivines that crystallized from magmas. Roedder (personal communication) in a preliminary review of our observations believes that both host and inclusions can be explained as being derived from a magma. We suggest an alternate hypothesis—that the glassy inclusions were frozen liquid droplets incorporated into olivine, which itself did not crystallize from a magma. Following are several reasons for this suggestion:

1. Single and relatively large olivine crystals in the matrix are not associated with any other adhering crystalline material. A meteorite type consisting of only olivines (most of which are practically Fe-free) and contain melt inclusions is unknown.

2. Aggregates of olivine grains that may contain glassy inclusions are loosely consolidated. This state of aggregation appears contrary to a magmatic origin.

3. We have noted olivines with inclusions within 1–2 mm chondrules in the Allende C3 meteorite. The inclusions are similar in appearance to those in olivines from both igneous rocks and to those in Murchison. Similarity in appearance, however, does not necessarily signify a common mode of origin. Clearly, chondrules solidified as discrete systems of millimeter dimensions and did not crystallize in a magma chamber.

4. The C2s, next to the C1s, contain elemental abundances that approximate solar abundances. Most, if not all, of the components of C2s must have condensed from primordial matter. Thus, their silicates and metal must have been closely associated with a condensation process and not with a fractionating magma. Further implications of this condensation process will be discussed later in the summary.

Poorly Characterized Phases

Two ubiquitous minor phases are present in all polished sections studied. Both are soft and exhibit a dull beige color in reflected light, but they differ considerably in form and mode of occurrence. The first of these is massive in appearance, mottling is usually present, masses are optically isotropic though sometimes showing faint undulatory extinction. Characteristic shapes observed vary: (1) regular spheres resembling chondrules, (2) angular to irregular pieces with serrated edges (Figure 8a), and (3) irregular rounded blebs (Figure 8b). The first two are most often found within the matrix, while the blebs occur within or between olivine grains in white inclusions. Based on shape alone, the blebs might have replaced preexisting metal where it was exposed to attack along fractures or grain boundaries. It is typical that metal securely protected within olivine shows no alteration. On the other hand, isolated blebs of this

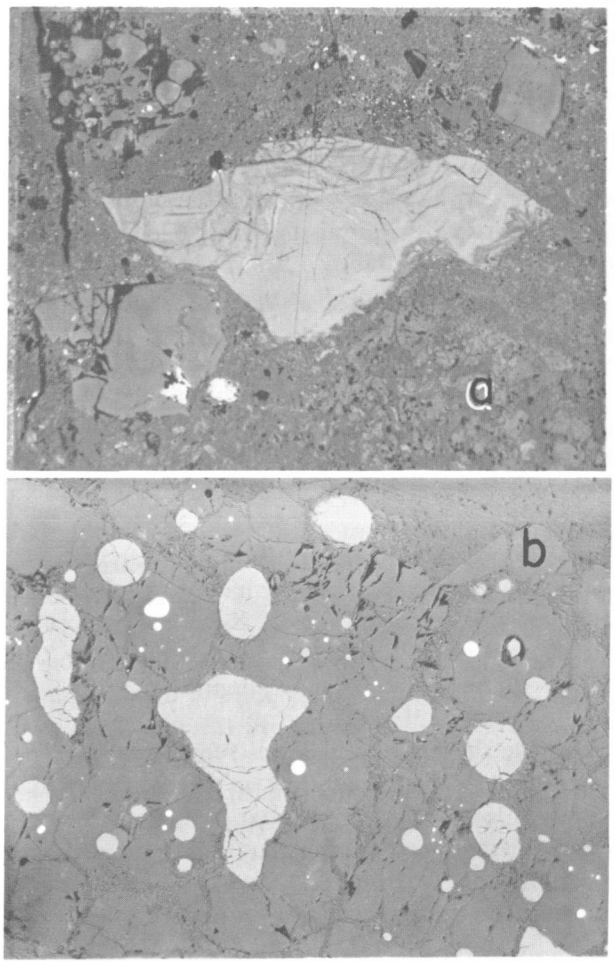

FIGURE 8.—Various shapes of massive Fe-S-O phase: *a*, irregular form (0.3 mm long) in Murchison matrix. Note the variegated texture and what appear to be drying cracks; *b*, oblate and oval forms in granular olivine inclusion. Smaller bright spots are metal. Width of field is 0.5 mm.

massive phase show no channel fillings leading to them. If metal within these inclusions were the precursor, then the replacement must have occurred prior to incorporation of the inclusions in Murchison, since unaltered metal coexists within the matrix. As can be seen from the photographs, what appear to be drying cracks are usually present. Blebs of this phase can sometimes be removed easily from white inclusions; they are highly magnetic and give no X-ray powder pattern. The overall weak magnetism of the matrix material of Murchison may be due to inclusions of this phase.

In occurrences (1) and (2) above, the edges of these masses are slightly corroded and embayed. This could represent either of two things: direct reaction with the matrix material or reaction with some liquid or gaseous phase that, at some time in the preterrestrial history of the meteorite, passed through the permeable, fine-grained matrix and attacked this phase or some preexisting phase. Most of the masses show diffuse edges which may represent more advanced stages of reaction. This massive phase occasionally contains minute blebs of metal or troilite and pentlandite.

In a few instances patches of a highly anisotropic phase consisting of a criss-cross matting of fibers or plates (5 to 10 microns long) are contained within an isotropic groundmass resembling the massive phase. This fibrous or sometimes platy phase is the second poorly characterized phase seen in Murchison. Some typical occurrences are shown in Figure 9.

The anisotropy and reflectivity of these fibers in polished sections approaches that of graphite and may easily be mistaken for it. X-ray patterns show one sharp line at 5.4 Å and a weaker line at 2.72 Å. The pattern could not be identified.

It is not clear if these two phases are related. It is possible the massive material represents an alteration of the fibrous material, or the converse, that the fibers represent a crystallization from the amorphous phase. On the other hand a cluster of fibers do occur alone within the matrix in one instance, and in several other instances clusters of fibers were found rimming and projecting into large calcite crystals (Figure 9c). The fibers are clearly much lower in abundance than the massive, amorphous phase.

Many of the properties we have noted for these poorly characterized phases resemble those de-

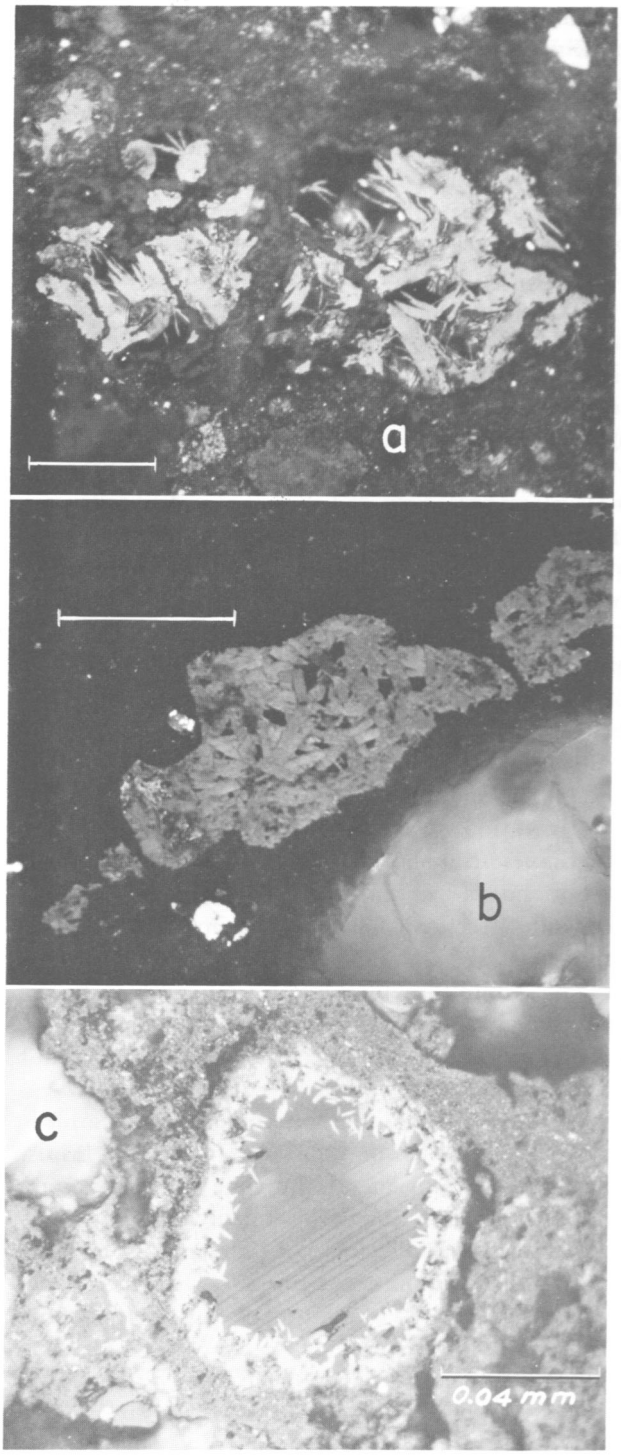

FIGURE 9.—Photographs of unidentified highly anisotropic fibrous and platy phase. Oil immersion, reflected light: *a*, fibers and plates embedded in matrix. Scale bar is 20 microns; *b*, interlocking plates within matrix. Scale bar is 20 microns; *c*, fibers within and bordering polysynthetically twinned calcite crystal.

scribed for several types of an unknown phase (or phases?) noted by Prof. Ramdohr (1963) in the Mighei C2 meteorite. He suggested that it might be a new Fe-C-S mineral with low Ni content and that its low hardness indicated a layered structure. Our X-ray results for the fibrous or platy phase would appear to confirm a layered structure, but we have not attempted to gather any compositional data because of the narrow width (1–2μ) of the fibers and platelets. Our probe results for the massive phase indicates a more complicated composition.

Averaged microprobe results for the massive phase are, in weight percent (with ranges, where available, in parentheses): S 17.6 (16–19), Fe 42.0 (37–45), Ni 6.1 (5.9–8.2), Cr 1.6 (1.4–2.5), C 0.2, P. 0.3, O 31.0, sum = 99.7. Approximately fifteen areas of this phase on two separate probe sections were analyzed. Wavelength scanning showed no other elements present in detectable amounts (specifically no Cl, F, or Mg and only a faint trace of Si). The fact that the sum is close to 100% is fortuitous, as our accuracy for oxygen was low. The result for oxygen may at best be semiquantitative, but even this is significant. The stoichiometry does not fit that of any known oxysalts of sulfur: the atomic Fe+Ni+Cr to sulfur ratio is 1.6, whereas most known compounds are unity or less. Some hydrated oxysulfates exist with similar stoichiometries but none close enough to draw any conclusions. This massive phase was determined to be water insoluble, hence it does not contribute to the soluble sulfate content of the bulk chemical analysis of Murchison.

Regardless of what kind of compound this represents, the association of Fe with both Ni and Cr make it impossible to postulate a simple alteration of troilite or pentlandite.

In the heating experiments on the matrix material described earlier ("X-ray Evidence" and Table 4), we note that this fibrous phase appeared to break down to troilite. The steps in the reaction could not be followed; they could involve reaction with the surrounding matrix rather than straight thermal decomposition.

Textural Features

In the "General Description" we distinguished four distinct inclusion types. Each of these types exhibits features that bear upon the preterrestrial history of the whole meteorite.

Type 1 Inclusions

This type of inclusion consists of (1) fragmental pieces and single crystals of individual minerals contained directly within the black matrix, and (2) individual mineral phases that appear to have grown within the black matrix. In the first category the minerals are clearly debris that was incorporated into the matrix. In all, these debris fragments comprise approximately 8 vol. % of the meteorite.

The majority of type 1 inclusions are in the first category above, and are represented by euhedral and angular olivines, angular pyroxenes, angular chromites, and angular pieces of glass. Minerals in the second category are calcite, gypsum, magnetite, and the two poorly characterized phases noted earlier.

The olivines and pyroxenes vary in composition from grain to grain, and a small percentage of the olivines are moderately to strongly zoned. A microprobe grain count of the homogeneous (i.e., unzoned) olivine and pyroxene fragments indicates a ratio of olivine to pyroxene of approximately 2/1. The olivine fragments average larger in size than the pyroxenes so the actual volume ratio will be larger than this. Histograms of these olivine and pyroxene compositions are given in Figure 10. The diagrams are closely similar to the ones determined by Fredriksson and Keil (1964) for the Murray meteorite. Wood (1967a) made an extensive survey of this kind for all inclusions in ten C2 chondrites. He discussed some subtleties in the distribution from one meteorite to another; however, the overall patterns are the same as for Murchison.

Figure 11 illustrates a special grain to grain survey that was made on an unusually metal-rich section. Grains of olivine not associated with grains of metal show the same kind of histogram as just discussed above. Olivines associated with metal, however, show an absence of fayalitic compositions. Fredriksson and Keil (1964) suggested for the Murray C2 meteorite that metal was formed by a Prior's Rule—type of process by reduction of the fayalitic component of olivine to form metal and the more forsteritic olivine. As compelling as this argument

is, it meets with some serious mass balance problems. In Murchison, for example, a fayalitic olivine of 30–40% Fa contains about 0.1% NiO (Figure 18, and "Nickel in Olivines"). Reduction of the FeO and NiO from this olivine would yield associated metal containing only 0.4% Ni, which is over an order of magnitude smaller than that observed in any C2 meteorite (Wood, 1967). Metal in Murchison, for example, ranges from 4% to 7% nickel. Thus, the nickel balance does not work out. In addition, the ratio of masses of metal to forsterite in associated grains shows wide variation with, in extreme cases, grains consisting of up to 50% (by vol.) of metal. It appears that reduction in situ does not account for the metal-olivine associations. It would appear more likely that they are the result of the initial condensation process from the solar nebula. As will be discussed in the summary, depending on the total (hydrogen) pressure, metal condensation accompanies or slightly precedes the condensation of the first forsteritic olivine. Thus, metal grains would be associated with, and possibly acting as nuclei for, the precipitation of forsterite. As condensation continues metal ceases to form, while small amounts of more fayalitic olivine, not associated with metal, condenses.

Fragments of zoned olivines were found that showed zonal variations from as little as 5 mole % Fa to as much as 40 mole % Fa. It should be noted, however, these results are largely from frag-

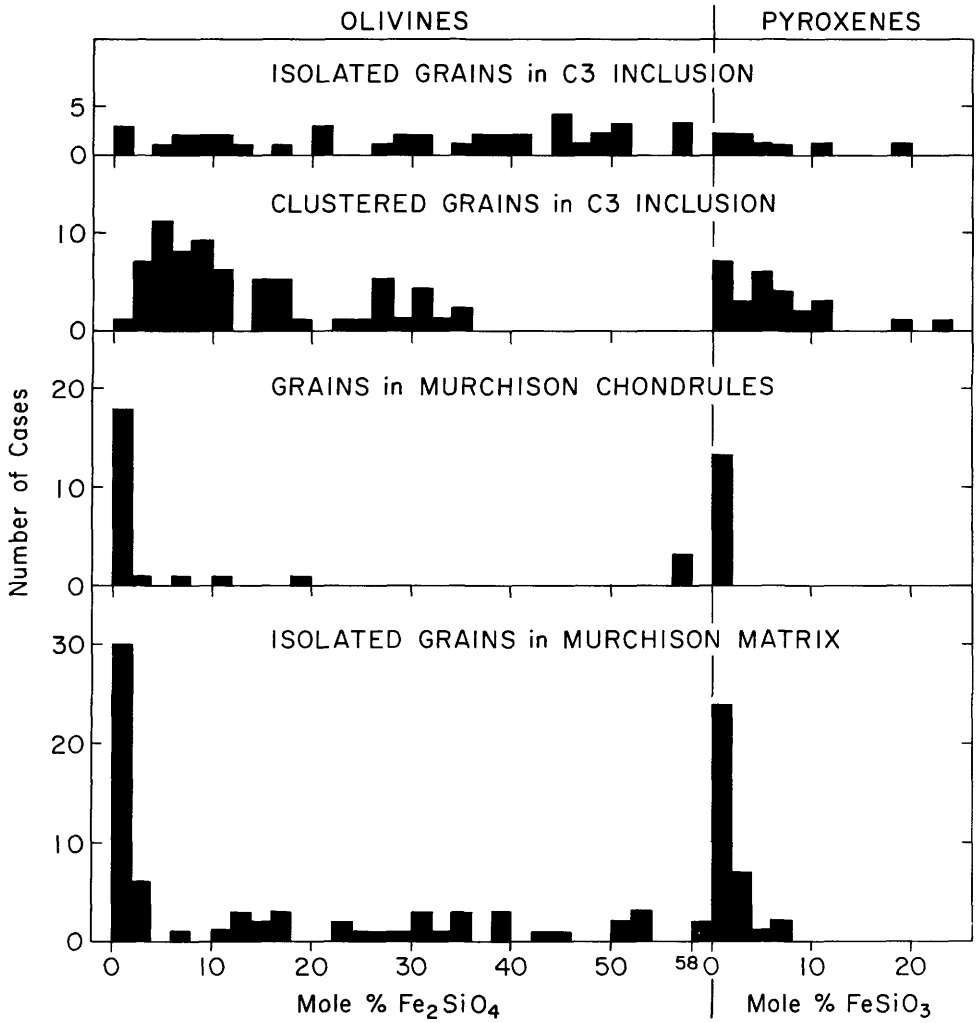

FIGURE 10.—Histograms of olivine and pyroxene compositions. A few more Fe-rich compositions (up to Fa_{55}) are omitted for brevity.

ments so that it is impossible to determine what is rim and what is core, or indeed if the full variation of the original crystal is represented in the fragment that was encountered. In many cases fayalite values did not show a concentric arrangement but a monotonic change from one Mg-rich edge across the fragment to the opposite Fe-rich edge. Such asymmetric changes show that Fe-rich edges cannot be the result of interaction with the high iron matrix material. In some instances, however, concentric symmetry was observed with a Mg-rich center and Fe-rich rims. In a few rare cases reverse zoning was observed, with cores more Fe-rich than the rims!

One of the striking features observed in this type of inclusion is the presence of rare whole single crystals of olivine in the matrix (Figure 12). In many instances these crystals are perfectly euhedral, showing a full set of terminating faces. They range in size from 0.3 mm to 1 mm and are either equant in shape or somewhat flattened prisms. This is, as far as we know, the first reported occurrence of this phenomenon in any C2 chondrite. Specimens of Murray and Cold Bokkeveld we examined, however, exhibited the same kinds of olivine crystals. It may be this is a characteristic feature of other C2 chondrites. In some instances, otherwise perfect crystals are broken or chipped. The crystals are never attached to other grains but are isolated in the matrix such that their removal leaves behind a

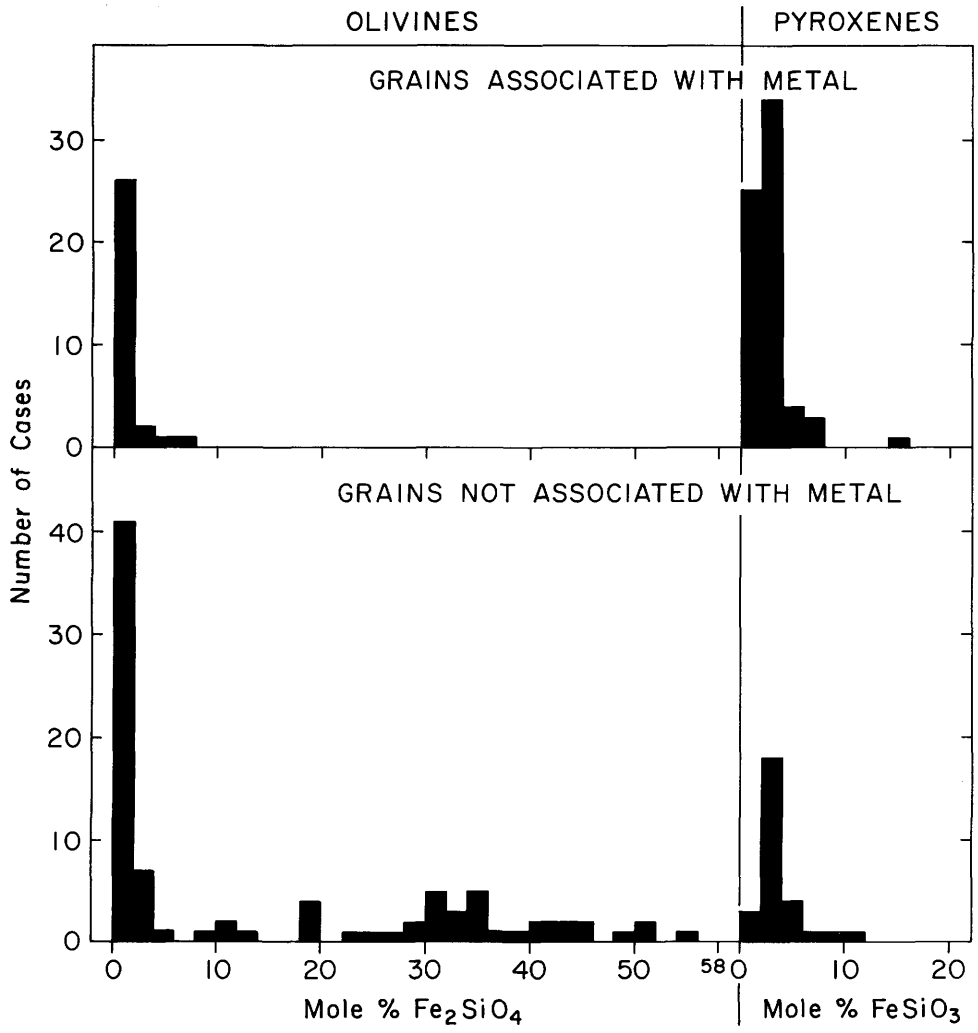

FIGURE 11.—Histograms of olivine and pyroxene compositions in Murchison. These data were obtained on a metal-rich section different from that used for Figure 10.

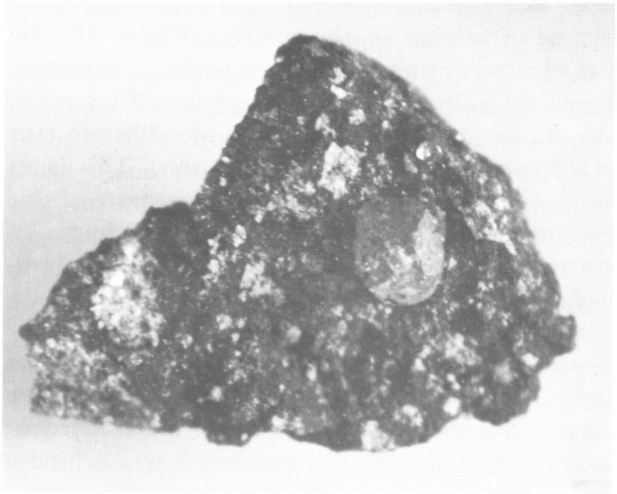

FIGURE 12.—Euhedral olivine crystal (0.5 mm) embedded in matrix.

smooth-walled negative crystal cavity. An interesting feature of these crystals is that the faces always appear slightly frosted.

Some of these crystals are zoned. Measurements of four of them showed core to rim values from Fa 25 to Fa 45, 3 to 8, 22 to 31, and 23 to 35. Other crystals, however, were unzoned and showed consistent compositions of less than Fa 1. Of the crystals that were selected for microprobe work and study a few contained internal blebs of glass (up to 36 microns), spherules of metal, and euhedral crystals of spinel. These glass inclusions were described in detail under "Glasses."

It is clear these euhedral crystals did not form within the matrix. Olivine is not a mineral that develops crystal faces against impeding matrix as do minerals like staurolite and garnet. Euhedral olivines are found in terrestrial rocks only in instances where they crystallize within a melt (e.g., magnesian olivines poikilitically contained in pyroxene or plagioclase in some basalts, troctolite, or peridotites) or subhedral crystals projecting into open cavities (as fayalitic olivines in some volcanic obsidians and trachytes, or coarse gabbro pegmatites). Furthermore, some of the fragments of olivine within the Murchison matrix show several crystal faces still present on them. These were originally fully euhedral crystals that were broken and then incorporated into the black matrix. We believe it highly likely that *all* of the angular olivine fragments (most of which show no crystal faces) are pieces of larger, once euhedral, crystals. Only a small percentage of the olivine crystals managed to be incorporated into the Murchison matrix before being fragmented.

Single crystal X-ray patterns made of these euhedral olivines are extremely sharp, indicative of a high degree of order and, by inference, relatively slow cooling. They are clearly not quench products.

TYPE 2 INCLUSIONS

The most prominent inclusions in Murchison are these so-called "white inclusions." Because they tend to be rounded in outline, they are frequently called "chondrules" by casual observers. Closer study, however, clearly distinguished them from true chondrules, and the presence of true chondrules in Murchison (type 3 inclusions) further accentuates the distinction.

"White" is somewhat of a misnomer. The great majority of the inclusions are snow-white, however, a few are blue or spinach green. Type 2 inclusions range in size from approximately 0.5 mm to 4.5 mm and are generally rounded to elliptical in cross section, though a high proportion of them have intricate, crenulated or lobate outlines (Figure 13). In a few hand specimens we observed a large number of elongated lenslike shapes that showed a slight lineation pattern suggestive of solid flow.

The boundaries of type 2 inclusions are generally sharp, although on a fine scale grains at the edges jut out into the black matrix. Often the matrix rimming an inclusion is unusually black and fine grained. In no case is it possible to work loose one of these inclusions from the matrix and remove it as a whole unit, as can be done with true chondrules.

Most of the type 2 inclusions are quite granular in texture, the grains being only loosely packed together. A needle gently raked over the surface of one easily produces a small pile of grains. Most of these inclusions consist of clusters of anhedral to subhedral grains of usually more than one phase. The dominant phase is highly magnesian olivine (Figure 10), and it is present in almost all of these inclusions. In rare instances, however, inclusions are found that contain no olivine at all.

The most common inclusion consists of sugary

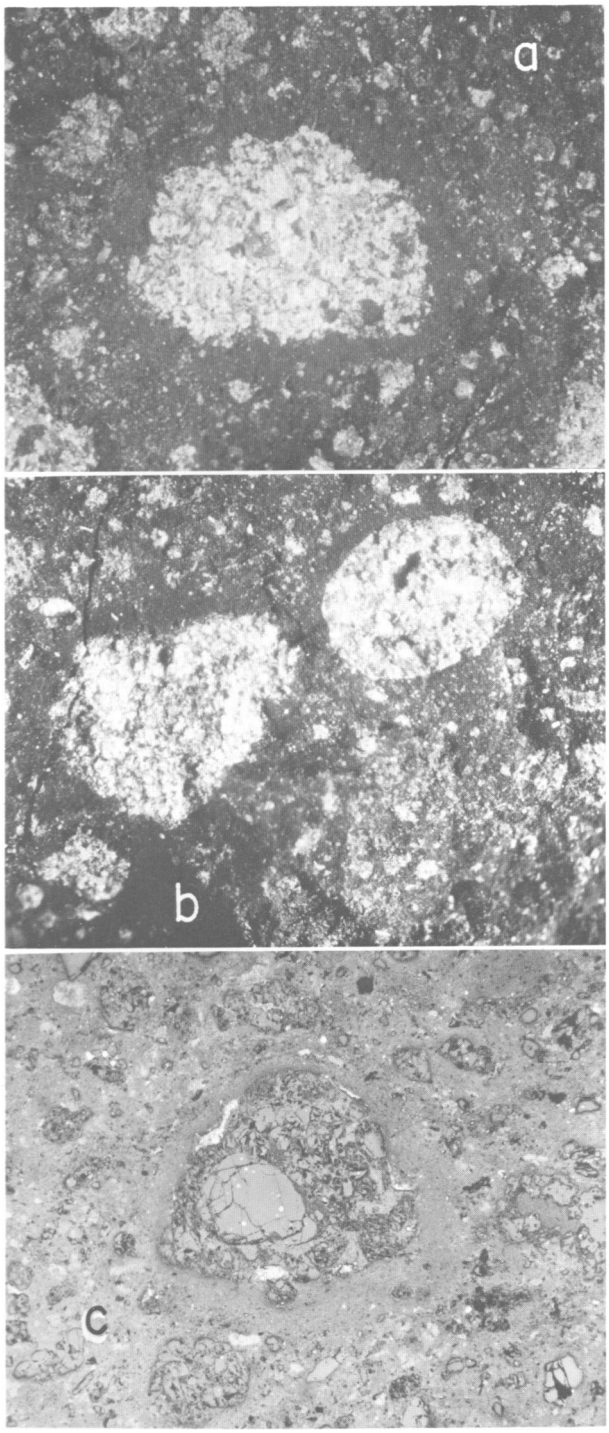

FIGURE 13.—Typical white inclusions in matrix: *a*, inclusion (1.7 mm wide) surrounded by a narrow band (0.2 mm wide) of fine-grained, inclusion-free matrix; *b*, two white inclusions, each is surrounded by a narrow band of fine-grained matrix. Long dimension of oval-shaped inclusion is 1.7 mm; *c*, polished section showing granular white inclusion surrounded by fine-grained matrix. Width of field is 1.5 mm.

textured, granular, white forsterite which may contain blebs of metal. Within a given inclusion the forsterite shows some variations in composition from grain to grain. The average variation we have observed is from Fa 1 to Fa 5, although in a few instances fayalite contents up to Fa 60 were observed. Accessory spinel, calcite, diopside, troilite, pentlandite, whewellite, and chromite may be present as intergranular phases in type 2 inclusions.

Some of these inclusions contain appreciable amounts of low calcium pyroxene with the olivine, and in some instances the pyroxene exceeds the olivine. Other, less abundant, inclusions consist of white forsterite laced through with flakes of the spinach phase (layer-lattice silicate; see "Other Layer-Lattice Silicate"). In a few cases such inclusions exhibited the peculiar, regular interleaved olivine-spinach texture noted earlier, in which it is possible to break the plates of olivine and spinach from each other like separating pages of a book. A small number of inclusions consisted entirely of clusters of the spinach phase. We did not, however, observe a full range of proportions from all olivine to all spinach. The spinach was, in all cases, iron-rich (approximately 30% FeO), while the coexisting olivine was generally iron-poor. It is, therefore, not possible to derive the spinach (a mixture of polymorphs of chamosite ± serpentine) from in situ hydration alteration of the olivine without invoking an improbable sequence of cation additions and subtractions.

A very small number of white inclusions contained no olivine but consisted of spinel with calcite, or spinel with clinopyroxene. The former represented the largest sizes of white inclusions ever seen in the meteorite, up to 4.5 mm across.

Finally, blue patches in white inclusions (approximately 0.15 mm), consisting mainly of hibonite, perovskite, and spinel with or without diopside, were found in trace amounts. These high temperature Ca-rich assemblages were described and discussed in detail under "Hibonite" and "Perovskite."

TYPE 3 INCLUSIONS (TRUE CHONDRULES)

True chondrules are in low abundance in Murchison. Because they do not break with the matrix, it is relatively easy to distinguish them. They stand out as spherical or ellipsoidal projections on

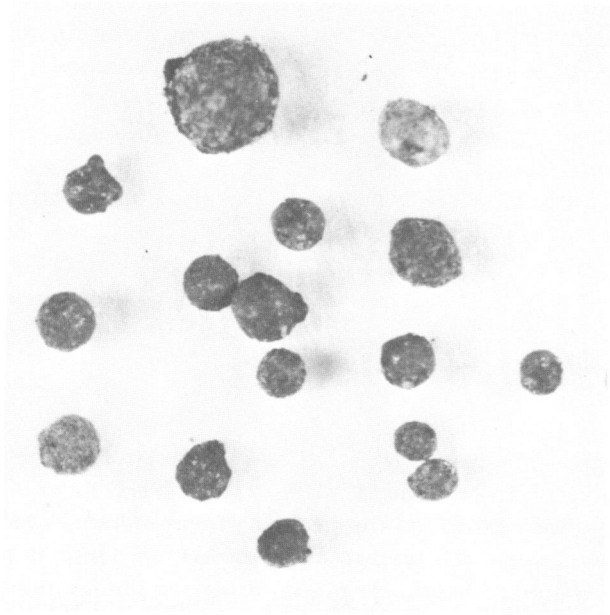

FIGURE 14.—Assorted true chondrules which were easily separated from matrix. Largest shown is 0.75 mm in diameter.

fresh fracture surfaces and can, with care, be worked loose and removed (Figure 14). The majority of the chondrules are dark gray to black on the outside, although in a few instances very small (0.1 mm and smaller) pure white spheres occur in the matrix.

The white spheres are mechanically weak and break open at attempts to remove them from the matrix. Internally they consist of very fine-grained, silky white shreds of either clinoenstatite or orthoenstatite (almost iron-free) with minor olivine and calcite sometimes present. X-ray patterns of the orthoenstatites showed disordered or ordered forms in individual instances (Pollack and Ruble, 1964).

The more common black chondrules ranged from 0.05 to 0.8 mm in diameter. Separated individual ones were mounted and sectioned. These consisted of a variety of internal textures and mineralogies. Mostly they contained olivine as granular aggregates of subhedral to anhedral grains surrounded by streaks of glass, or stringers of the spinach phase layer-lattice silicate. Small patches of the poorly characterized (Fe-S-O) phase are peppered through some individual chondrules. Ca-poor pyroxene was found but is rare. A microprobe survey of olivine and pyroxene compositions shows most of the olivine to be close to pure forsterite with a few more iron-rich compositions, and a small peak at Fa 58–59 (Figure 10). This peak is due to one single chondrule that contained this composition of olivine as scattered subhedral crystals within a matrix of a pigeonitic pyroxene (approximately Fs 50) that contains stringers of glass. Compositions within individual chondrules were uniform.

Most chondrules contained some minor specks of sulfide and metal, and few were quite rich in metal with blebs of 50 to 150 microns. Individual metal grains are uniform in composition, but the nickel content did vary somewhat from grain to grain within individual chondrules, from 4.5 to 5.7% Ni. One chondrule contained a single metal grain that ran 9.6% Ni.

Many of the chondrules contained from minor to major amounts of irregular patches, blebs, and streaks of glass that were quite variable in composition from point to point. Microprobe analyses show it to be a high Ca-Al-silicate glass that is alkali-poor. The compositions are all within the range of values for the glass found in type 1 inclusions (Table 8).

Some unique chondrules were found. One consisted almost entirely of the poorly characterized (Fe-S-O) phase discussed earlier. Another consisted of small subhedral to anhedral grains of olivine (Fo 99) surrounded by massive spinach layer-lattice phase (Table 2b). Once again it is clear that the layer-lattice phase could not be derived by direct hydration alteration of virtually Fe-free olivine because of the high iron content of the layer-lattice mineral. Another chondrule was seen that contained a fairly large, lobate void space cavity. Small cavities were evident in several others; however, we could never be certain they had not been created during the sectioning process by the plucking out of small metal grains. The large cavity, however, is an original feature by virtue of its unique shape and size.

It is clear that the individual true chondrules represent much of the same range of chemical conditions as observed in the types 1 and 2 inclusions described earlier. One significant difference, however, is the smaller number of different mineral species found in the true chondrules in contrast to the white inclusions, especially the very high temperature phases such as perovskite, hibonite, and spinel, which were not observed in any true chondrule.

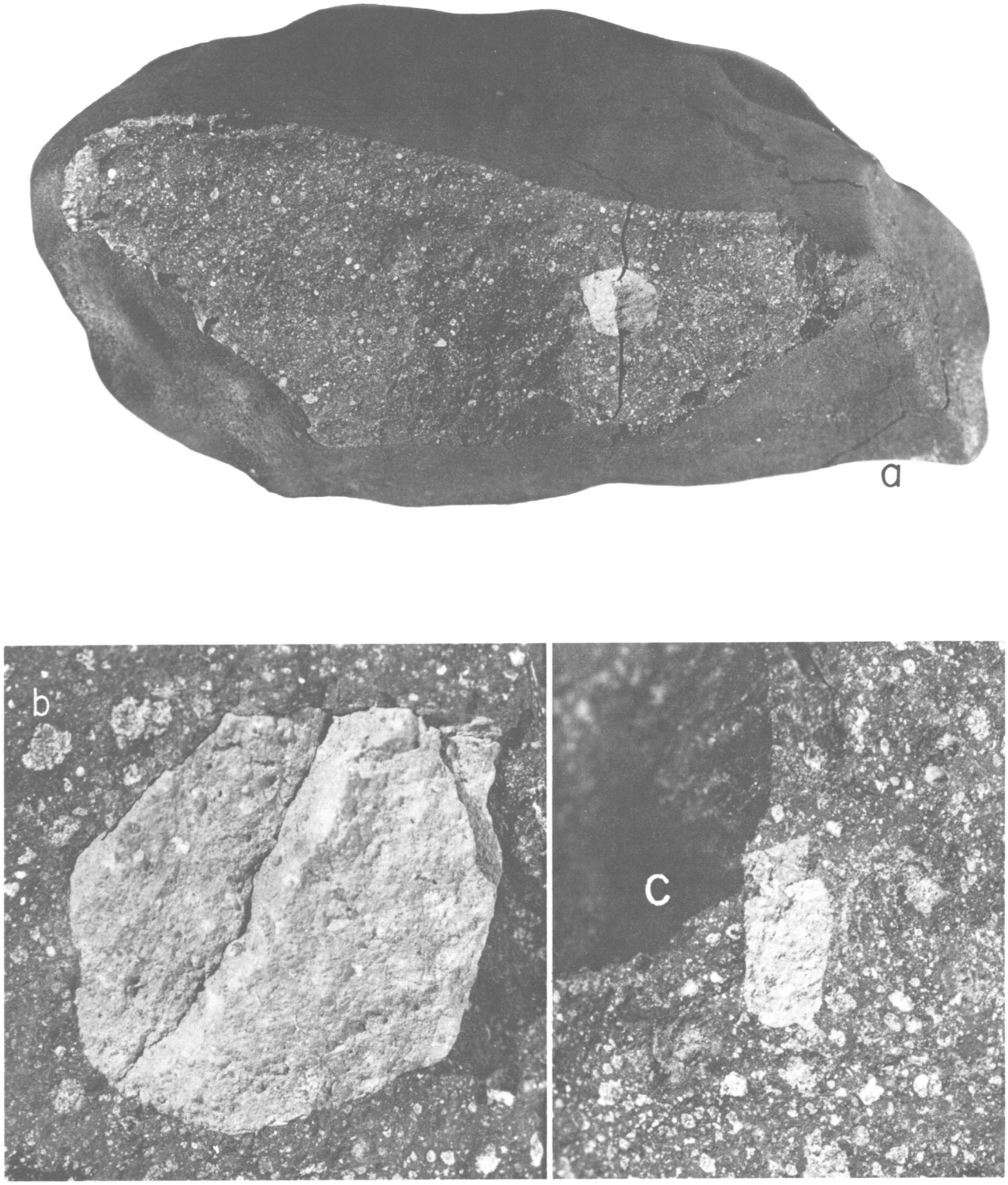

FIGURE 15.—C3 xenolithic inclusions in Murchison: *a*, largest fragment found is 1.3 cm in diameter and is contained in an 18–cm picce of Murchison; *b*, close-up of same fragment (note the thin separation of fragment from surrounding matrix); *c*, smaller (7 mm) xenolithic fragment of same C3 meteorite type found in another sample of Murchison.

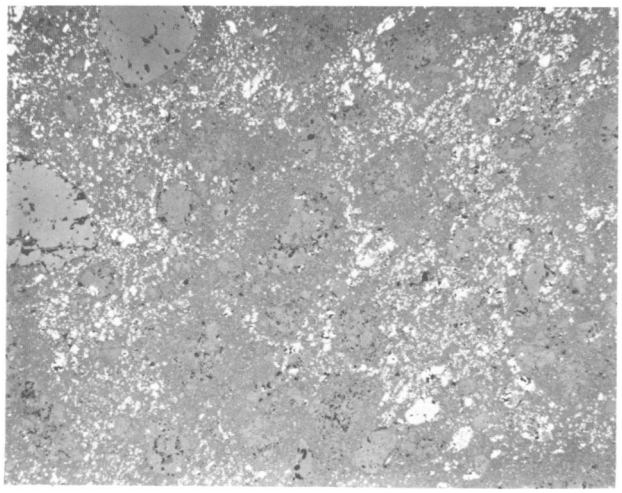

FIGURE 16.—Polished section of C3 inclusion (type 4) shown in Figure 15*b*. All bright spots are troilite or pentlandite. This unusually high-sulfide-containing inclusion is practically metal free. Width of field is 1.5 mm.

It is significant that among the chondrules collected and studied from Murchison, not one is like the common chondrules of the ordinary chondrites: barred olivine, radiating pyroxene-plagioclase, porphyritic olivine. Furthermore, the glass within Murchison chondrules is very different in its range of compositions from the sodium-rich glasses of the chondrules in ordinary chondrites.

TYPE 4 INCLUSIONS (XENOLITHIC FRAGMENTS)

Within Murchison we encountered xenolithic fragments of two other different meteorite types: (1) six fragments of one meteorite type, ranging from a few millimeters up to 13 mm (Figure 15); and (2) a single fragment, 1.2 mm, of yet another meteorite type (Figure 17).

C3 CHONDRITE INCLUSIONS.—Fragments of this meteorite type are a distinctive light blue-gray color. The largest fragment is slightly separated from the surrounding matrix such that it could be completely removed as a unit. Within these fragments we observed both distinct true chondrules and inclusions, the latter with the same morphologies as the type 1 and type 2 inclusions found in the body of Murchison proper.

The main matrix of these xenolithic pieces consists of finely comminuted, submicron size olivine and pyroxene with numerous coarser irregular patches of abundant troilite and pentlandite (Figure 16), and a trace of ilmenite and magnetite. Nothing can be said about the matrix olivine and pyroxene compositions; they are too fine-grained for microprobe analyses.

Contained within this matrix were inclusions that consisted of single phase angular fragments, rounded pieces, anhedral, subhedral, and (rarely) euhedral grains of mainly olivine, with lesser Ca-poor pyroxene. The only metal seen in any xeno-

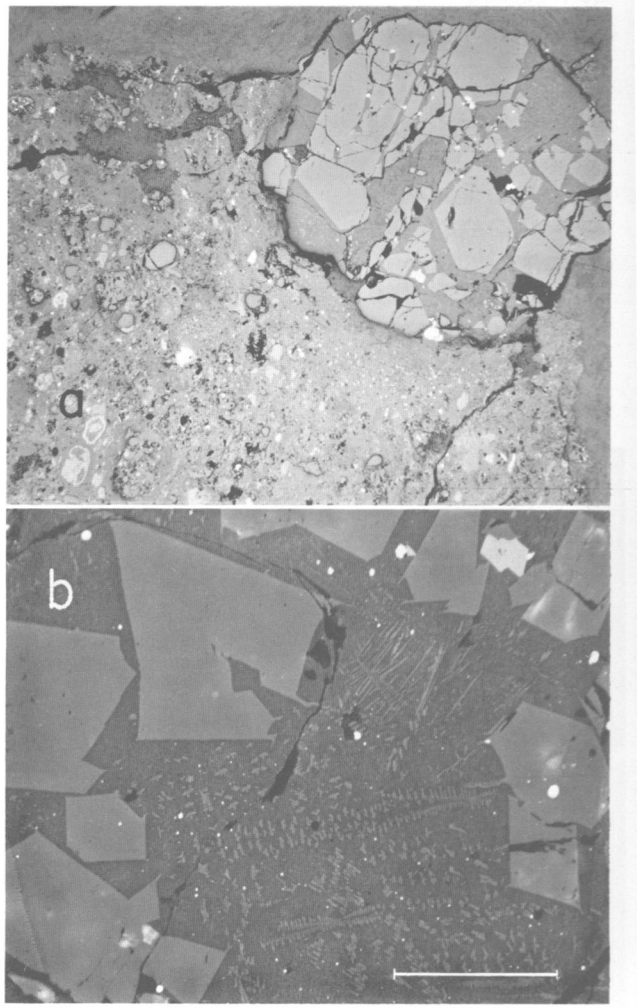

FIGURE 17.—Second type of xenolithic inclusion in Murchison: *a*, inclusion shown in upper right is 1.2 mm in diameter and contains large euhedral crystals of olivine (Fo_{100}) in a partially devitrified groundmass (note contrast in texture with Murchison matrix); *b*, enlarged area of inclusion showing devitrified glass groundmass. Large crystals are olivine, small euhedral crystal is chromite (lighter gray), bright spots are metal and sulfide. Scale bar is 100 microns.

lithic fragment occurred as two micron-size grains in an olivine inclusion.

In addition, inclusions of multigrained aggregates of olivine, pyroxene, minor sulfide, and a minor unidentified phase were found. All of these inclusions appear analogous to the type 1 and type 2 inclusions seen in Murchison proper.

The olivines and pyroxenes in these xenolithic fragments show wide compositional variations from grain to grain with, however, a different distribution of compositions than in Murchison proper (Figure 10). Many of the grains are zoned. Olivine zones ranged from Fa 2–20 to Fa 51–57, with all combinations of values between. Pyroxenes ranged from Fs 2–8 to Fs 15–22, with other values in between.

Most of the inclusions in the xenolithic fragments were rimmed by nonopaque, ultra fine-grained matrix (of submicron olivine and pyroxene) that is virtually free of sulfides and coarser grained silicate fragments.

True chondrules are present in the xenolithic fragments; however, they are rare. Only a few were observed on the largest fragment. No detailed study was made of them.

It is worthwhile to highlight the complete absence of any layer-lattice silicate in the xenolithic meteorite fragments. At the contacts of the fragments with the surrounding Murchison matrix there is a complete break, with no interfingering of layer-lattice material into xenolithic fragments. Thus it is impossible that the hydrated layer-lattice phases in Murchison proper are derived from the alteration of olivine in situ. If that were the case then the olivines in the xenolithic fragments would have been pervasively altered also, or at least attacked at their rims in contact with Murchison proper. The very smallest xenolithic fragments (approximately 1 mm) show just as sharp boundaries with the black matrix of Murchison as do the larger ones.

In addition, the xenoliths contain no other low temperature phases like those observed in the surrounding Murchison proper: calcite, whewellite, gypsum, poorly characterized phases.

Macroscopically these appear to be xenoliths of a C3 chondrite. Comparisons were made with specimens of a number of C3s, of both the Ornans and Vigarano subtypes (Van Schmus, 1969). In general appearance the fragments looked more like the Ornans subtype; however, the very high ratio of matrix to inclusions plus chondrules and the nonopacity of the matrix material contrast markedly with the Ornans-subtype as examined by us directly and as described and characterized by Van Schmus.

Furthermore the almost complete absence of metal, and the abundance of sulfides adds to the problem of comparison. Sulfides make up about 7 vol. %, half of which was troilite and the other half pentlandite.

A partial wet chemical analysis was performed: Mg = 14.5%, Fe = 25.2%, Ni = 1.55%. Mason (1971) noted some chemical groupings of Vigarano and Ornans subtypes on a plot of Mg against Fe. A plot of the values given above lies exactly between the two groupings as illustrated in Mason's paper. On this basis it is not possible to put it distinctly into either group.

In the histograms of olivine compositional variations for C3 subtypes presented by Van Schmus (1969), these xenolithic fragments (Figure 10) show their main peak at 5–10 mole % Fa, which is similar to the Kainsaz meteorite in the Ornans subtype group.

We conclude that the xenolithic fragments in Murchison are of a C3 chondrite that is similar to the Ornans subtype in terms of olivine-pyroxene compositional distribution, is intermediate between the Ornans and Vigarano subtypes in terms of the bulk composition, and is unlike either subtype in terms of texture.

G. Mueller (1966) noted the presence of an angular xenolithic inclusion in Mighei C2 chondrite. Megascopically it appeared similar to a C3 chondrite. It was, however, a darker colored fragment and contrasted less markedly with the surrounding Mighei matrix than the fragments in Murchison (G. Mueller, pers. comm.). It is possible that C3 inclusions in C2 meteorites is more widespread than heretofore imagined.

Xenolith of Unknown Meteorite Type.—One section of Murchison contains a single small (1.2 mm) xenolithic fragment of a second meteorite type (Figure 17). It consists of blocky, jointed pieces (some subhedral crystals) of pure forsterite set in a matrix of glass, with traces of troilite, metal, and euhedral chromite. The glass is partially devitrified into a dendritic pattern of submicron needles.

In texture and mineralogy this fragment is identical to a unique chondrule observed and photo-

graphed by Ramdohr (1966) in the Adelie Land ordinary chondrite (L5). He referred to it as an "unknown (or nearly so) type" of chondrule. This occurrence in Murchison may be a fragment of this rare type of chondrule.

Mineralogical-Compositional Relationships

In studying the Murchison meteorite a number of relationships were observed between mineral phases and between compositional components of individual mineral phases, which bear on the history of the meteorite.

Calcium in Olivines

Weight percent CaO was obtained for a group of 21 olivines, of which 17 were homogeneous and 4 were zoned. These were chosen at random and included olivines in both type 1 and type 2 inclusions. Fayalite contents ranged from 0 to 85, with a distribution like that shown in Figure 10. CaO contents ranged from 0.08 to 0.77%. No correlation exists between CaO and fayalite contents for the homogeneous olivine grains. For the zoned olivines one crystal showed a positive correlation: CaO increased from 0.15 to 0.48% as fayalite content increased from 54 to 85. The other zoned crystals, however, show constant CaO contents in all zones regardless of fayalite content. As an example, CaO = 0.26% as fayalite goes from 36 to 48. Fredriksson and Keil (1964) observed no CaO-fayalite correlation in olivines of the Murray C2 chondrite.

Chromium in Olivines

Twelve random olivines (9 homogeneous, 3 zoned) were analyzed for Cr_2O_3 values. These ranged from 0.06 to 0.3 wt. %. Homogeneous olivines showed no correlation between chromium and fayalite contents. Similarly, chromium remained constant across all zones in zoned crystals (e.g., Cr_2O_3 = 0.3% for fayalite from 25 to 35).

Manganese in Olivines

Thirteen random olivines (9 homogeneous, 4 zoned) were analyzed for MnO. These ranged from zero to 0.3 wt. %. Although there was a slight tendency for MnO to increase with fayalite content, the data were too few to draw a definite conclusion. Such a correlation would be likely because of the closely similar behavior of iron and manganese in most sets of conditions. Terrestrial (crustal) and most meteoritic conditions would not be expected to show any substantial difference in this trend (Simkin and Smith, 1970).

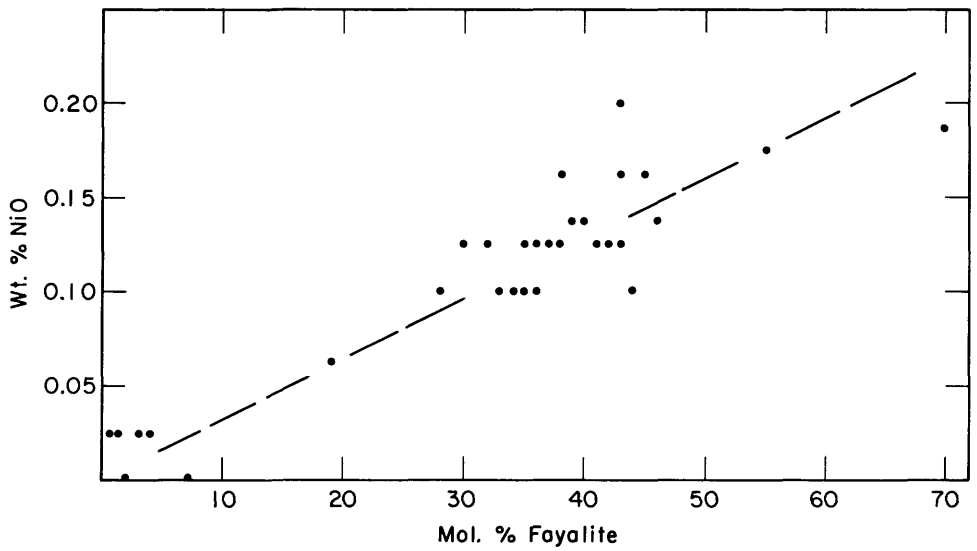

Figure 18.—NiO vs fayalite content in olivine grains in Murchison.

Nickel in Olivines

Nickel analyses were performed on 31 olivines randomly selected from one polished section of Murchison (Figure 18). A correlation exists: NiO increases with the fayalite content. As fayalite goes from essentially zero to 80 mole percent, NiO goes from less than 50 ppm up to 2300 ppm. There is some scatter to the data, part of which is analytical error, and a smaller portion of which is due to errors in always returning to the same grain to analyze for both Fe and Ni, since both were done on the same microprobe spectrometer channel, with all the Fe counts obtained first. The correlation is, nevertheless, quite evident and is exactly opposite to the correlation observed in terrestrial rocks by Simkin and Smith (1970).

The explanation of the opposite correlation is clear from the calculations of R. Mueller (1965) in the system Fe-MgO-SiO_2-O_2. In terrestrial rocks, olivines (and coexisting pyroxenes) coexist at equilibrium with ferrite phases such as magnetites or chromites but not metal. With *increasing* oxidation state the fayalite content of the olivine *decreases* as iron is oxidized from the + 2 to the + 3 state into ferrite phases. Since the oxidation potential of nickel beyond the +2 state is extremely high it becomes progressively enriched in the olivine in which it forms an ideal solid solution (Campbell and Roeder, 1968). Thus, Mg-rich terrestrial olivines contain more NiO as observed by Simkin and Smith (1970).

In a more reducing environment than the terrestrial crust, at oxygen partial pressures less than those of the ferrite-metal boundary, just the reverse happens. With *decreasing* oxidation state the fayalite content of the olivine (and pyroxene) *decreases* as iron is reduced into the metallic state (or a reduced sulfide phase such as troilite). Because the oxidation potential of nickel from the +2 state to the neutral state is higher than that of iron (from +2 to neutral), nickel is more readily reduced than iron. Thus, for oxidation states that do reduce iron, nickel is reduced along with it. As the oxidation state drops the olivine becomes more Mg-rich and poorer simultaneously in nickel.

It is clear from studies on equilibrated chondrites that the fayalite content decreases with lower oxidation state and that Mg-rich (Ni-poor) silicates, such as olivines and pyroxenes in iron meteorites, olivines in pallasites, and pyroxenes (and rare olivine) in enstatite chondrites and enstatite achondrites, represent reduced environments (and generally higher temperature environments than more oxidized meteorites). The olivine and pyroxene fragments found in the matrix of Murchison clearly did not originate there in equilibrium with each other (because of the large grain to grain variations in composition, and the clastic texture of these inclusions). They represent a variety of oxidation conditions. By virtue of the correlation we observe (Figure 18) these conditions were established in equilibrium with metal and not in equilibrium with the ferrite phases which occur in small amounts also in the matrix and inclusions of Murchison. On the basis of the kind of condensation sequence which formed the minerals of Murchison, metal and olivine formed closely together in temperature, while ferrites formed about 1000°C lower. This condensation sequence will be discussed in detail in the summary (also cf. Table 9).

Figure 19 is a plot of the NiO content in olivines from one of the xenolithic fragments of the C3 chondrite found in Murchison. It shows the same trend as for Murchison proper. From our earlier description (C3 Chondrite Inclusions) this meteorite is also disequilibrated and clastic-textured. The almost complete absence of metal and the high amounts of troilite and pentlandite indicates it is

TABLE 9.—Equilibrium condensation sequence of phases observed in Murchison (total pressure 10^{-3} atm) *

Phase	T°C (rounded values)
Hibonite	1500 (approx.)
Perovskite	1375
Spinel	1240
Metal	1200
Diopside	1180
Forsterite	1170
Enstatite	1075
Intermediate compositions of olivines and pyroxenes	700-250
Troilite (+ pentlandite)	425
Magnetite	130
Layer-lattice phases	<150
Poorly-characterized phases	<<100
Whewellite	<<100
Calcite	<<100

* Most data after Grossman, 1972. Temperatures of phases condensing below 150°C (except magnetite) are estimated by the authors.

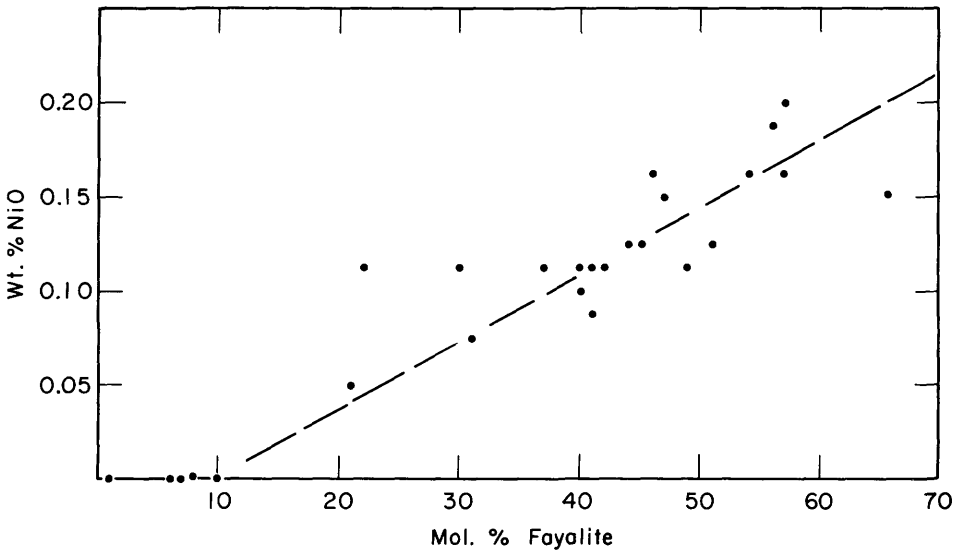

FIGURE 19.—NiO vs fayalite content in olivine grains in C3 xenolithic inclusion.

an agglomeration of grains from a higher sulfur environment than for Murchison proper. Thus, most of the iron and nickel reduced out of the silicate phases (for the Mg-rich reduced compositions, which dominate the histogram, Figure 10) went into iron and nickel-rich sulfide phases.

NICKEL IN PYROXENES

In doing the survey of NiO in olivines of Murchison, pyroxene grains were also examined. No detectable NiO was found in any of them. This is logical in view of the histogram (Figure 10): virtually all the pyroxenes are very Mg-rich, hence very reduced and thereby Ni-poor.

CHROMIUM AND PHOSPHORUS IN METAL

The high Cr and P contents of the metal grains are different from all known meteoritic metal analyzed thus far. It is similar to some of the metal grains from the lunar samples, though they never reach the values observed in Murchison metal. Superficially it would appear that the metal represents somewhat more reducing conditions than for other meteorites, and that Cr and P were alloyed into early-forming metal rather than coming out in lower temperature Fe- and Cr-rich spinels and silicates, and phosphates, respectively. Certainly the fact that almost all the metal occurs as included beads within very iron-poor olivine would tend to bear this out. On the other hand, the metal shows no detectable Mn or Si. The latter would require extreme reduction such as observed in the Horse Creek iron or in the enstatite chondrites. Mn, however, would be expected to be reduced into the metal along with Cr and P. Its solar abundance (Goles, 1969) relative to Fe is about the same as P and is only a factor of two less than Cr. In this regard, metal in enstatite chondrites (Keil, 1968), though notably high in Si, shows no Cr or P of unusual significance. We are currently investigating the metal in a large sampling of carbonaceous chondrites and hope to be able to draw conclusions in a later paper. For the time being we have no solution to the unusual compositions of the metal grains in Murchison.

MINERALS NOT PRESENT IN MURCHISON

Perhaps as significant as the minerals that have been found is the absence, or only trace presence, of minerals common to the ordinary chondrites: plagioclase feldspar, chromite, ilmenite, or phosphates such as whitlockite. All sections of Murchison were searched carefully for these and only chromite was found in traces. Ilmenite was found

as a trace within one of the C3 xenolithic inclusions, but not in Murchison proper.

Wet Chemical Analysis of Murchison

As in overall appearance, so too in bulk chemical composition, Murchison is closely similar to Murray. The results obtained are shown in Table 1a and compared with the published data of Jarosewich (1971). These data are also compared on a volatile-free (C, H, N, O, S) basis in Table 1b. On this basis the agreement between the major constituents is better since the effect of our larger H_2O (–) value is eliminated. Jarosewich has kindly supplied a sample of his analyzed material to allow for a comparison of some of the analytical results (especially Na and Fe) on the sample. These data follow:

	Jarosewich	*this work*	
SiO_2	29.07	28.95	
Fe (total)	22.15	21.73	
	22.29	21.73	
MgO	19.94	19.94	
		20.01	
Na_2O	0.23	0.21	(flame emission)
		0.21	(atomic-absorption)
H_2O (total)	10.05	9.66	
C (total)	2.12	1.96	

Analysis by Jarosewich of two separate portions of our sample confirmed our high Na value. We have further investigated this point by determining Na in five separate interior fragments from five different pieces of Murchison and found that the Na_2O content ranged from 0.19% to 0.71%. The weighted average was 0.48%. Sodium in our analyzed sample is relatively high and variable. Such a result could be due to contamination after fall or to the fact that sodium is indeed heterogeneously distributed in this meteorite.

We have not assigned values for FeS, FeO, and Fe_2O_3 in our analysis for the following reasons:

1. Sulfide sulfur is estimated by subtracting the sum of elemental and sulfate sulfur from the total sulfur content. There is a tendency for both the elemental and sulfate sulfur values to be low due to incomplete extraction of the elemental sulfur by carbon tetrachloride or of sulfate sulfur by hot water. This results in a high estimate of sulfide sulfur.

2. As described earlier an appreciable amount of sulfur is present as the so-called poorly characterized Fe-S-O phase, rather than as FeS. Also some sulfur is present as pentlandite.

3. Mineralogical examination by point-counting on polished sections shows that the total sulfide content is much less than that calculated by subtracting elemental and sulfate sulfur from the total sulfur. Point-counting of four sections gives troilite + pentlandite ranging from 0.07% to 0.23% by weight (average 0.13%).

4. Earlier, in the discussion of the layer-lattice matrix material, crystal-chemical considerations indicated an appreciable amount of ferric iron in the matrix other than that due to the minute amount of magnetite. These facts, along with the inherent errors in the estimate of FeS make the assignment of iron as FeO difficult.

Summary and Discussion of Observations

Many of the foregoing observations bear out what has been described in C2 meteorites by others (DuFresne and Anders, 1962; Wood, 1967; Mason, 1962–63 and 1971). Some of the observations, however, are new and raise questions regarding interpretation and how they fit into existing schemes of carbonaceous chondrite genesis. Four of these will be summarized and discussed in this section.

First, it has been recognized for some time that C2 meteorites possess a high temperature fraction contained in a matrix of low temperature material. The high temperature fraction is generally considered to be forsterite with some enstatite and spinel. In addition to this assemblage we have observed two other high temperature fractions: the perovskite-hibonite-spinel-(±)diopside assemblage; and blebs of Ca-Al-silicate glasses, of variable compositions, contained within olivine (and occasional spinel) crystals.

The perovskite-hibonite-spinel-(±)diopside assemblage is closely similar to the assemblage observed in some C3 chondrites (Fuchs, 1971; Keil and Fuchs, 1971); in contrast to them, however, no gehlenite or anorthite was found. In Murchison the assemblage is very rare and is not found with the frequency it is in such C3s as Allende. The fact that it is present *at all* in a C2 is significant, and together with the glasses it provides a partial answer to the question raised by Mason (1971) re-

garding the mineralogical form of Ca and Al in C2 meteorites.

The sequence of direct condensation of crystalline solids from a solar nebula was originally computed by Lord (1965), later recomputed by Larimer (1967), and most recently recalculated with a revised scheme by Grossman (1972). Because of the lack of thermodynamic data on hibonite no calculation includes it in the crystallization sequence, although an educated guess would place its stability in the 1350°–1450°C range (Grossman, 1972). In Grossman's calculation, at a total gas (primarily hydrogen) pressure of 10^{-3} atm, perovskite condenses out at 1374°C, followed by melilite and spinel at 1352°C and 1240°C, respectively. Melilite does not occur in Murchison; however, the association of diopside with spinel could represent the breakdown products of melilite by later reaction with gas at 1177°C, or the bypassing (metastably) of the melilite field. Forsterite and enstatite do not appear until 1171°C and 1076°C, respectively. Thus, the perovskite-hibonite-spinel-(±)diopside assemblage, though minor in quantity, clearly represents a higher temperature stage than heretofore observed in any C2 meteorite. It may actually occur in other C2s, but not yet recognized.

Whether metal precedes, accompanies, or follows the condensation of forsterite depends on variations in the total (hydrogen) pressure, with less than an order of magnitude controlling the sequence (Grossman, 1972). In Murchison, most of the metal occurs *within* olivine crystals, indicating pressures above 10^{-4} atm where the metal condenses before forsterite. The euhedral morphology (cf. Textural Features) of many of the forsterite crystals suggests condensation from a vapor phase. Metal grains must have acted as preferred nucleation sites for some of the olivine because the high surface tension of metal surfaces makes them ideal nuclei. The few zoned olivines represent disequilibrium with the gas with falling temperature.

The form of the metal grains within olivine crystals is always spherical or subspherical blebs, or lobate clusters of two or more blebs. The shapes strongly suggest the metal was originally present in liquid drops. This has also been noted by Wood (1967b), who drew the same conclusion. The shapes contrast sharply with the angular metal grains and occasionally stringy metal veins of the ordinary chondrites. In experimental systems iron condensed from the gas phase usually forms elongate crystals and needles. The textural suggestion of a liquid phase for the metal in Murchison is further raised by the Ca-Al-silicate glass inclusions that are relatively abundant within olivines (and some spinels).

As noted in "Glasses" under "Mineralogy," these glass bleb inclusions vary in composition and occasionally contain void space bubbles (Table 8, Figure 7). In one instance a single bleb was found that consisted of two glasses of different compositions. Compositionally, the average glass computes to normative anorthite and diopside with excess silica. In a solar nebula condensation (at 10^{-3} atm total pressure) crystalline anorthite should condense out at 1089°C, after forsterite, but before enstatite. The mineral anorthite readily crystalizes in experimental systems and does occur in the high temperature fraction of some C3 chondrites, as well as in euhedral to subhedral crystals in some achondrites.

The presence of glasses of these compositions within olivines and some spinels in Murchison points to an early liquid stage. As discussed in the section on glasses, one possibility is that the glass inclusions represent trapped blebs of a coexisting rest-magma from some magmatic stage in a planetary object. We noted there, however, four major difficulties with postulating a magmatic state that requires complicated, highly contrived conditions that are contrary to the primitiveness of a meteoritic object such as Murchison. It appears more reasonable to suggest that these glasses are part of the normal formational processes that condensed primitive solid matter in the solar system, as many others have suggested (e.g., Anders, 1971), rather than a magmatic stage on some early planetary object.

The variability in the compositions of the glass blebs clearly indicates that they were not formed in a single event, or stage, sampling a homogeneous solar nebular composition.

The distinct indication of a liquid phase raises the question whether the spherical habit of the metal grains in olivines might also represent original liquid drops. Since liquid metals cannot be quenched to glasses, as can most silicate liquids, there is no way to decide other than to point to the morphology.

Wood (1963) raised the question of condensation

of solar nebular matter initially into a liquid stage. The idea was generally discarded when it became clear that unreasonably high total pressures would be required for the solar nebular gas, of the order of 10 to 10^3 atmospheres (Anders, 1971). Recently, however, Turekian and Clark (1969) have invoked total pressures in the range of 0.1 to 1 atm as a means of accounting for density differences and differences in accretion histories among the terrestrial planets, Mercury, Earth, and Mars. Toward the center of the primitive solar nebula both pressure and temperature would increase (Cameron, 1962).

Although two of the glasses in Murchison reach 7.5% and 9.4% MgO, they are all much too depleted in it. Thus, they are fractionated relative to nebular abundances. Formation of liquids of these compositions at pressures of 1 atm or more would require temperatures in the range of 1350-1450°C, as noted under "Glasses." In a condensation of these liquids from the solar nebular gas they may be the compositions that liquefy first. With activity data for the elements in liquids in these compositional ranges, a calculation of the first liquid composition to condense is possible. Such calculations are currently in progress by M. Blander (personal communication).

The most logical sequence to account for these glasses, as well as the apparent initial liquid droplets of metal, would be for direct condensation of liquids near the center of the solar nebula, at pressures and temperatures commensurate with the formation of silicate and metal liquids. Turbulent conditions and solar-flare activity could cause variation in the compositions of small regions of space as well as the necessary fluctuations in pressures to cause liquids to form. The majority of these drops did not survive but, with falling pressure, were resorbed into the gas phase. Some very small droplets did survive, however, and were moved outward in the ecliptic plane. There, with falling pressure and temperature, additional resorption into the gas phase would occur until the droplets became cool enough to act essentially as solids, or at least develop a surface skin that would inhibit reevaporation. Hoyle (1960) described the process of separation of an ecliptic plane disk of matter from the proto-sun, and the transfer of angular momentum to it. He calculated that early condensed matter could easily migrate outward away from the inner part of the disk, as long as the condensed matter does not accrete into objects above 100 cm in diameter.

Thus, these tiny quenched drops could move outward into less turbulent regions where, Hoyle estimates, the average pressure of matter in the gaseous disk is 10^{-3} atm. Here the droplets that survive become incorporated into the dominant early condensing solids, forsterite and spinel.

Attractive as this scheme is, it still requires at least transient pressures of above 100 atm, held long enough to allow some droplets to condense. In addition, as noted under "Glasses," some of the liquid blebs are deformed from spherical shapes and consist of elongated blebs that lie parallel to crystallographic directions in the olivine crystals in which they are contained. This would mean that the glass drops would have to remain plastic and deformable while the temperature fell 200°C (from approximately 1350°C, where the glasses condense, to 1170°C at which forsterite sublimes), and the pressure fell five to six orders of magnitude (10^2 or 10^3 down to 10^{-3} atm).

An alternative scheme would be for the earliest crystalline phases, like perovskite, melilite, spinel, hibonite, diopside, to condense from the solar nebula at equilibrium gas pressures of 10^{-3} atm, and then suffer a high transient heat, such as suggested by Whipple (1966) and Cameron (1966). This would melt the particles already condensed, and they would quench to a metastable state as glass droplets, later to be incorporated into olivine once the normal sequence of equilibrium condensation resumed. The major problem with this scheme is that no combination of solids that condense from the solar gas at temperatures above that at which forsterite condenses can form glasses of the compositions that were measured (Table 8). The silica content is plainly too high.

This leads us to the interesting approach of Blander and Katz (1967), in which they established an argument that the kinetics of nucleation processes favor the metastable nucleation of liquid drops initially, at pressures of 10^{-3} to 10^{-4} atm. These would form by supersaturation of the nebular gas, component by component, as subcooling took place below the temperatures where equilibrium solids should have crystallized out. Under such

a regime, variability in compositions among the droplets of liquid would be a direct consequence. Furthermore, droplets formed by such a non-equilibrium process could maintain their plasticity, stiffening only when they survive to lower temperatures (i.e., below the glass transition temperature). As such, they could become nuclei for forsterite and spinel that later crystallized via equilibrium condensation from the gas, and in individual cases still be plastic enough to become crystallographically elongated within the forming olivine. Under conditions of supersaturation, metal would be expected to form spherical to subspherical grains also; this would happen even if the metal condensed directly to a solid state. Blander (personal communication) states that iron vapor can be subcooled as much as 300°C before condensation.

This treatment of Blander and Katz offers many attractive advantages in explaining these glasses in Murchison. The only disadvantage is the lack of quantitative thermodynamic data for the liquids at the present time. For the supersaturation condensation process to work for Murchison, about 100 to 200°C (at 10^{-3} atm) of subcooling would be required. Blander (personal communication) believes this amount is probable in this process.

Second, details of the accretion process are, of course, matters of interest and speculation. We observed that the white (type 2) inclusions are almost always surrounded by thin rims of exceptionally black matrix material (Figure 13). The deep blackness is due to the complete absence of light-colored grains of olivine, pyroxene, etc. These inclusions typically do not have a great deal of mechanical integrity, as noted earlier. They appear to have clumped together into commonly ellipsoidal, but occasionally irregular, masses before incorporation into the accreting Murchison parent body. The low temperature, submicron size (smoke) layer-lattice material appears to have coated the white masses forming the thin, black rim. In a hard vacuum, surface-attractive forces of newly formed layer-lattice phases, with high surface area per unit mass, would be quite "sticky." The formation of the adhering film of layer-lattice material would act to seal each clump of coarser grained silicates and allow each of them to act as a unit until incorporation into the accreting body. Even at that the low mechanical integrity of the white (type 2) inclusions shows that the accretion process for the parent body of Murchison must have been an exceedingly gentle process; clumps of silicates, smoke-size layer-lattice particles, true chondrules, single crystal grains and grain fragments, and fragments of at least one other body (type 4 xenolithic inclusions) must have been moving with near zero relative velocities, otherwise the white inclusions would never have survived. Indeed, the single grains of silicates in the matrix (type 1 inclusions) may be, in part, the remains of white clusters that were disaggregated in the accretion process.

Third, it is worthwhile to reemphasize our observation of the peculiar form of green (spinach) layer-lattice silicate that occurs as regular interleaved plates within forsterite grains (described under "Other Layer-Lattice Silicate" and "Type 3 inclusions") (Figure 3). It should be noted that these easily separable green plates are not connected to the exterior black matrix material. DuFresne and Anders (1962) observed this spinach phase within olivine in Murray and from it concluded that olivine was pervasively altered by hydration, and these represented the process caught short of completion.

As we have shown in great detail earlier the layer-lattice phase (or phases) is not a simple chemically hydrated equivalent of olivine. In addition, we wish to emphasize here the importance of the type 4 inclusions (xenolithic fragments). These fragments were clearly derived from other accreted objects that were fragmented, dispersed, and later incorporated into the Murchison body. If pervasive hydration-alteration then attacked almost all of the Murchison olivine to form the layer-lattice material, these olivine-rich xenolithic inclusions should have been altered also; they are not. In addition, Onuma et al. (1972) on the basis of his oxygen isotope work found "no direct genetic relationship between any pair of the three fractions: matrix [i.e., layer-lattice material], high-iron olivine, and low-iron olivine." Clearly, the layer-lattice material formed in space as a low temperature condensate at under 150°C (Anders, 1971; Onuma et al., 1972) and accreted into a body, accompanied by high temperature mineral fragments and xenolithic fragments.

The development of the green plates of spinach within olivine may be related to strings of elongated glass blebs arranged in parallel rows within

condensed olivine crystals. If these glasses were considerably more Mg- and Fe-rich, and Ca- and Al-poor, than the glasses discussed earlier they could have been attacked at low temperatures (below 150°C) when the fine, smoke-size particles of layer-lattice matrix material were condensing. Water was the major oxygen-bearing, gas-phase component, and it preferentially attacked these glass layers within olivine. Such Mg- and Fe-rich, Ca- and Al-poor glasses would have formed at somewhat lower temperatures than the other glasses that did survive within olivine crystals. It is, in our opinion, highly unsatisfactory to postulate the existence of a glass that is now completely destroyed in order to account for the peculiar olivine-spinach texture shown in Figure 3. Nevertheless, it is clear that the textural relation between high temperature olivine and the low temperature, layer-lattice spinach phase, together within single grains, must precede the accretion of the host olivine into the parent body. We have shown earlier that the alteration could not have taken place after accretion, otherwise other olivines, both in the matrix and in the xenolithic inclusions, would have been altered also.

Fourth, by whatever process the mineral components of Murchison condensed (i.e., by equilibrium condensation or by nonequilibrium subcooling-supersaturation-condensation), there was a more or less continuous fractionation of mineral phases as the nebular gas temperature fell. If we use the equilibrium condensation model (as computed by Grossman, 1972) plus estimates from other sources (e.g., Onuma et al., 1972) as bases *for comparison only,* then the estimated range of temperatures for the entire mineral assemblage observed in Murchison would be as shown in Table 9. Clearly, a range is represented from very high to very low temperatures, and statements made in the literature in the past that C2 meteorites consist of *a* high temperature fraction and *a* low temperature fraction are somewhat misleading. What is meant, obviously, is that the most abundant minerals are the forsterites and the layer-lattice material; all others are relatively minor in quantity. This frequency distribution might be interpreted as a rapid drop in temperature from the 1000°C range to the 150°C range, but is more likely a function of bulk composition of the nebular gas and its state of oxidation with falling temperature. Clearly the cooling was rapid enough that early formed higher temperature phases did not adjust their solid solution compositions continuously with falling temperature; a small percentage developed zoned overgrowths instead. The puzzling feature of the sequence of minerals in Murchison is the complete absence of feldspar phases, which should appear (under the perfect equilibrium situation) in the 1100°C–700°C interval. Their absence may be due to the same kinetic factor that kept olivine and pyroxene from adjusting compositions at lower temperatures. Most of the original Ca and Al are tied up in the early glasses and spinel. The metastable persistence of these with falling temperatures would not allow the gas to resorb enough of these elements to establish the correct composition for condensation of feldspars.

In summary, we consider that early-formed glass and metal condensed directly by a process like that described by Blander and Katz (1967), at pressures of approximately 10^{-3} atm and temperatures around 1200°C. Hibonite, perovskite, spinel, additional metal, forsterite, and enstatite formed by approximatedly equilibrium condensation shortly after, from 1200°C down, so as to poikilitically include the glass blebs and most of the metal within mainly forsterite crystals. All lower temperature phases formed by condensation that may or may not have been in strict equilibrium with the cooling gas, but might have involved subcooling, there is no way to tell. The most puzzling mineralogical aspects are the very low temperature phases. The spinach layer-lattice silicate and the poorly characterized Fe-S-O phase, together exhibit unusual textural relations with the high temperature phases, including low temperature partial replacement of them.

Restrictions on the thermal history of Murchison after final consolidation can be deduced from the stepwise heating experiments of the matrix material as reported in "X-ray Evidence." The maximum temperature at which no changes were detectable is 245°C. This compares favorably with thermometers proposed by others for different C2s. Mueller (1953) found this temperature to be 100°–350°C for Cold Bokkeveld based on the thermal decomposition of organic extracts. DuFresne and Anders (1961) give temperatures between 200° and 300°C for Mighei based on still other considera-

tions. Thus, reasonable agreement has been obtained for three C2s from different lines of evidence.

C2 meteorites represent very early, and very primitive, accreted matter. They may be less primitive than C1 meteorites. No sequence in time, C1–C2–C3, however, can be implied since Murchison contains well constituted xenolithic fragments of C3 meteorites. Clearly the formation of at least one C3 object preceded the formation of at least one C2 object in the time sense. This suggests that, although a time sequence between the carbonaceous chondrites does not apply, a spatial sequence must be the important factor. This would, in turn, indicate spatial fractionation and inhomogeneity with respect at least to volatiles (C, H, O, N) in the cooling solar nebula.

Note: As this manuscript was being typed, a paper, "Calcium Variations in Olivines of the Murchison and Vigarano Meteorites," by R. Hutchison and R. F. Symes, appeared in *Meteoritics*, 7: 23–29 (1972). Their results for the Ca contents in Murchison olivines are in accord with those reported here.

Appendix: Description of Wet Chemical Analytical Procedure

A 24-gram piece of the meteorite, free of crust, was ground in an agate mortar to pass 50 mesh. Portions of this material were taken for the several determinations.

H_2O- and SiO_2

These oxides were determined on one gram samples. The weight loss at 105°C was measured, after which the material was ignited, fused with sodium carbonate and silica determined by double dehydration with HCl, ignition to SiO_2 and volatization with HF. Silica in the combined filtrates was determined colorimetrically.

Total Fe, Ti, Mg, Al, Ni, Ca, Na, K, Cr, Mn, Co, and Cu Determinations

These elements were determined on aliquots of a solution of 6 grams of the ground sample. The sample was dissolved in a $HF–HCl–HNO_3–HClO_4$ acid mixture and evaporated to dryness. Repeated additions of perchloric acid and evaporation to near dryness with the final addition of a small amount of hydrochloric acid yielded a water-soluble residue that was diluted to volume. Aliquots of this "master solution" were used for the various determinations.

Total Fe, including Ti, was determined gravimetrically by preliminary precipitation with excess ammonia followed by precipitation of a HCl solution of the ammonia precipitate with cupferron. This precipitate was ignited to constant weight at 1100°C and weighed as $Fe_2O_3+TiO_2$. It was then dissolved in HCl, iron was separated from titanium by electrodeposition into a mercury cathode, and Ti was determined colometrically with peroxide.

Al, Mg, and Ca were determined on a second aliquot of the master solution. Aluminum was separated from iron by electrodeposition of the iron into a mercury cathode. It was separated from calcium and magnesium by a double ammonium hydroxide precipitation at pH 7. The hydroxide was dissolved in acid, evaporated to dryness, and heated to volatilize ammonium salts. Aluminum was then determined by the method of Watts (1958). Manganese was removed by the procedure of Peck (1964) prior to the calcium determination. Calcium was separated from magnesium by precipitation as calcium oxalate. The oxalate was ignited to the oxide, and this residue was dissolved and then titrated at pH 12.5 with 0.01 molar EDTA, using Acid Alizarin Black SN indicator (Belcher et al., 1958). Magnesium was determined by titration with 0.1 molar EDTA at pH 10 using Calmagite indicator in the filtrate from the calcium separation.

Cr, Mn, Cu, Co, and Ni were determined colormetrically on separate aliquots of the master solution. Chromium was oxidized to chromate and reacted with diphenylcarbazide. Manganese was oxidized to permanganate using periodate. Copper was reacted with Neo-cuproine (2,9 dimethyl–1,10 phenanthroline). Cobalt was reacted with Nitroso R salt and nickel with dimethylglyoxime after oxidation with bromine.

Na and K were determined in the master solution by atomic absorption spectroscopy (AAS).

Total Sulfur, Soluble Sulfur (SO_3), and Elemental Sulfur

Each of these was determined in a separate portion of the sample. For total sulfur approximately 1 gram of sample was sealed in a modified Carius tube with approximately 10 ml HCl and 0.5 ml $HClO_4$ and heated at 300°C overnight to disintegrate the sample and oxidize all sulfur to sulfate. The disintegrated sample was transferred to a Teflon beaker, HNO_3, HF, and HCl added, and the mixture evaporated to dryness to volatilize silica. After removal of iron by electrodeposition into a mercury cathode and a separation of aluminum by double precipitation at pH 7 with NH_4OH, sulfur was determined by precipitation as barium sulfate.

To determine soluble sulfur a 1 gm sample was leached for about 20 minutes with 150 ml of boiling water and then filtered and washed with about 100 ml of water. The filtrate was diluted to volume and sulfur determined gravimetrically as barium sulfate in a large fraction of the diluted filtrate. The remaining solution was shown by spectrographic analysis to contain Ca, Mg, Na, K, and Al. These elements (except K) were estimated more accurately by AAS and shown to be present in the molar ratios (with Na normalized to unity), 7.0 Mg: 2.2 Ca: 1.0 Na: 0.2 Al: 0.1 K*. These cations were equivalent to 87 percent of the sulfate found.

Elemental sulfur was extracted from the meteorite in a small Soxhlet-like extractor. After evaporation of the solvent the sulfur was oxidized to sulfate and determined gravimetrically as $BaSO_4$.

About one gram of the material was extracted for about 1.5 hours with 100 ml carbon tetrachloride. The solvent was then evaporated to dryness, oxidized with bromine, and sulfur determined. A blank was run on the carbon tetrachloride. The sample was then dried at 100°C and reextracted with 100 ml of carbon disulfide and sulfur determined in the residue after evaporation of the carbon disulfide. Most of the extracted sulfur found, 0.46%, was in the carbon tetrachloride extract while 0.025% was found in the carbon disulfide extract.

* K determined by spectrograph only.

Phosphorous Determined Colorimetrically as Molybdi-vanadophosphoric Acid

About 0.2 grams of the powdered material in a Teflon beaker was dissolved in a HNO_3–HF–$HClO_4$ mixture and taken to dryness. The residue, free of silica, was taken up in 6 *M* hydrochloric acid in 0.001 *M* sodium bromate, diluted to volume, and an appropriately sized aliquot passed through a small anion exchange column to adsorb iron. After rinsing sample from the column the eluate was evaporated to dryness, taken up in water, and phosphorous determined colorimetrically.

C, H, Total H_2O, and N

These were determined using a Perkin-Elmer carbon, hydrogen, nitrogen analyzer, Model 240. Relatively small samples, 10–15 mg., were taken for analyses. Ignition at 900°C was employed. An independent carbon determination was made on a 125 mg sample by ignition at 1100°C in oxygen and manometric measurement of the evolved carbon dioxide. This latter determination yielded a carbon content (1.91%) slightly higher than the value (1.85%) found using the analyzer at 900°C.

Estimation of Metallic Iron

About 0.75 gram of the sample was extracted with 3 grams of mercuric chloride in 150 ml of boiling water in a flask stoppered with a Bunsen valve for about 2 hours while magnetically stirred. The solution was then filtered through glass and iron determined colorimetrically in the filtrate.

Literature Cited

Ahrens, L. H.
1970. The Composition of Stony Meteorites (IX) Abundance Trends of the Refractory Elements in Chondrites, Basaltic Achondrites and Apollo 11 Fines. *Earth and Planetary Science Letters,* 10:1–6.

Anders, E.
1971. Meteorites and the Early Solar System. *Annual Review of Astronomy and Astrophysics,* 9:1–34.

Bass, M. N.
1971. Montmorillonite and Serpentine in Orgueil Me-

teorite. *Geochimica et Cosmochimica Acta,* 35: 139–148.

Belcher, R., R. A. Close, and T. S. West
1958. The Complexometric Titration of Calcium in the Presence of Magnesium: A Critical Study. *Talanta,* 1:238.

Blander, M., and J. L. Katz
1967. Condensation of Primordial Dust. *Geochimica et Cosmochimica Acta,* 31:1025–1034.

Boström, K., and K. Fredriksson
1966. Surface Conditions of the Orgueil Meteorite Parent Body as Indicated by Mineral Associations. *Smithsonian Miscellaneous Collections,* 151 (3) :1–39.

Brindley, G. W.
1951. Crystal Structures of Chamosites. *Mineralogical Magazine* 29:502–525.

Bunch, T. E., and K. Keil
1971. Chromite and Ilmenite in Non-chondritic Meteorites. *American Mineralogist,* 56:146–157.

Bunch, T. E., K. Keil, and E. Olsen
1970. Mineralogy and Petrology of Silicate Inclusions in Iron Meteorites. *Contributions to Mineralogy and Petrology,* 25:297–340.

Bunch, T. E., K. Keil, and K. G. Snetsinger
1967. Chromite Composition in Relation to Chemistry and Texture of Ordinary Chondrites. *Geochimica et Cosmochimica Acta,* 31:1569–1582.

Cameron, A. G. W.
1962. The Formation of the Sun and the Planets. *Icarus,* 1:13–69.
1966. The Accumulation of Chondritic Material. *Earth and Planetary Science Letters,* 1:93–96.

Campbell, F.E., and P. Roeder
1968. The Stability of Olivine and Pyroxene in the Ni-Mg-Si-O System. *American Mineralogist,* 53:257–268.

Carroll, D.
1970. Clay Minerals: A Guide to Their X-ray Identification. *Geological Society of America Special Paper,* 126: 80 pages.

Dodd, R. T.
1969. Metamorphism of the Ordinary Chondrites: A Review. *Geochimica et Cosmochimica Acta,* 33:161–203.

DuFresne, E. R., and E. Anders
1961. The Record in the Meteorites, V: A Thermometer Mineral in the Mighei Carbonaceous Chondrite. *Geochimica et Cosmochimica Acta,* 23:200–208.
1962. On the Chemical Evolution of the Carbonaceous Chondrites. *Geochimica et Cosmochimica Acta,* 26:1085–1114.

Ehmann, W. D., D. E. Gillum, J. W. Morgan, R. A. Nadkarni, T. Rabagay, P. M. Santoliquido, and D. L. Showalter
1970. Chemical Analyses of the Murchison and Lost City Meteorites. *Meteoritics,* 5:131–136.

Fredriksson, K., and K. Keil
1964. The Iron, Magnesium, Calcium, and Nickel Distribution in the Murray Carbonaceous Chondrite. *Meteoritics,* 2:201–217.

Freeman, E. S., and B. Carroll
1958. The Application of Thermoanalytical Techniques to Reaction Kinetics: The Thermogravimetric Evaluation of the Kinetics of the Decomposition of Calcium Oxalate Monohydrate. *Journal of Physical Chemistry,* 62:394–397.

Frondel, C.
1962. Ferroan Antigorite (Jenkinsite). *American Mineralogist,* 47:783–785.

Fuchs, L. H.
1968. X-ray Crystallographic Evidence for the Meteoritic Occurrence of Nepheline. *Earth and Planetary Science Letters,* 5:187–190.
1971. Occurrence of Wollastonite, Rhönite, and Andradite in the Allende Meteorite. *American Mineralogist,* 56:2053–2068.

Fuchs, L. H., K. J. Jensen, and E. Olsen
1970. Mineralogy and Composition of the Murchison Meteorite. *Meteoritics,* 5:198 [Abstract].

Goldstein, J. I., and A. S. Doan
1972. The Effect of Phosphorus on the Formation of the Widmanstätten Pattern in Iron Meteorites. *Geochimica et Cosmochimica Acta,* 36:51–70.

Goles, G. G.
1969. Cosmic Abundances. In Wedepohl, editor, *Handbook of Geochemistry,* 1:116–133, Berlin: Springer-Verlag.

Grossman, L.
1972. Condensation in the Primitive Solar Nebula. *Geochimica et Cosmochimica Acta,* 36:597–620.

Hoyle, F.
1960. On the Origin of the Solar Nebula. *Quarterly Journal of the Royal Astronomical Society,* 1:28–55.

Jarosewich, E.
1971. Chemical Analysis of the Murchison Meteorite. *Meteoritics,* 6:49–52.

Keil, K.
1968. Mineralogical and Chemical Relationships Among Enstatite Chondrites. *Journal of Geophysical Research,* 73:6945–6976.

Keil, K., and L. H. Fuchs
1971. Hibonite [Ca_2 (Al, Ti) $_{21}O_{38}$] from the Leoville and Allende Chondritic Meteorites. *Earth and Planetary Science Letters,* 12:184–190.

Kerridge, J. F.
1969. The Use of Selected-Area Electron Diffraction in Meteorite Mineralogy. Pages 500–504 in Millman, editor, *Meteorite Research.* Dordrecht, Holland: D. Reidel Publishing Company.

Kurat, G.
1967. Einige Chondren aus dem Meteoriten von Mezö-Madaras. *Geochimica et Cosmochimica Acta,* 31: 1843–1857.

Larimer, J. W.
1967. Chemical Fractionations in Meteorites. I: Con-

densation of the Elements. *Geochimica et Cosmochimica Acta,* 31:1215–1238.

Lord, H. C.
1965. Molecular Equilibria and Condensation in a Solar Nebula and Cool Stellar Atmospheres. *Icarus,* 4:279–288.

Lovering, J. F., R. W. LeMaitre, and B. W. Chappell
1971. Murchison C2 Carbonaceous Chondrite and Its Inorganic Composition. *Nature,* 230:18–20.

Mason, B.
1962–1963. The Carbonaceous Chondrites. *Space Science Reviews,* 1:621–646.
1971. The Carbonaceous Chondrites–A Selective Review. *Meteoritics,* 6:59–70.

Miller, C. C.
1953. Anhydrous Calcium Oxalate as a Weighing Form for Calcium. *The Analyst,* 78:186.

Morey, G. W.
1964. Phase Equilibrium Relations of the Common Rock-Forming Oxides Except Water. *U. S. Geological Survey Professional Paper,* 440–L:L70.

Mueller, G.
1953. The Properties and Theory of Genesis of the Carbonaceous Complex Within the Cold Bokevelt Meteorite. *Geochimica et Cosmochimica Acta,* 4:1–10.
1966. Significance of Inclusions in Carbonaceous Meteorites. *Nature,* 210:151–155.

Mueller, R. F.
1965. System Fe-MgO-SiO_2-O_2 with Applications to Terrestrial Rocks and Meteorites. *Geochimica et Cosmochimica Acta,* 29:967–976.

Onuma, N., R. N. Clayton, and T. K. Mayeda
1972. Oxygen Isotope Cosmothermometer. *Geochimica et Cosmochimica Acta,* 36:169–188.

Osborn, E. F., R. C. DeVries, K. H. Gee, and H. M. Kraner
1954. Optimum Composition of Blast Furnace Slag as Deduced from Liquidus Data for the Quaternary System CaO-MgO-Al_2O_3-SiO_2. *Transactions of the American Institute of Mining and Metallurgical Engineers,* 200:33–45.

Peck, L. C.
1964. Systematic Analysis of Silicates. *U. S. Geological Survey Bulletin,* 1170:66.

Pollack, S. S., and W. D Ruble
1964 X-ray Identification of Ordered and Disordered Ortho-Enstatite. *American Mineralogist,* 49:983–992.

Prince, A. T.
1954. Liquidus Relationships on 10 Percent MgO Plane of the System Lime-Magnesia-Alumina-Silica. *American Ceramic Society Journal,* 37:402–408.

Ramdohr, P.
1963. The Opaque Minerals in Stony Meteorites. *Journal of Geophysical Research,* 68:2011–2036.
1966. Observations on the Opaque Ore Content of some Meteorites, Especially from New South Wales. *Journal and Proceedings of the Royal Society of New South Wales,* 99:45–55.

Roedder, E., and P. W. Weiblen
1971. Petrology of Silicate Melt Inclusions, Apollo 11 and Apollo 12 and Terrestrial Equivalents. *Geochimica et Cosmochimica Acta,* Supplement, 2: 507–528.

Simkin, T., and J. V. Smith
1970. Minor Element Distribution in Olivine. *Journal of Geology,* 78:304–325.

Snetsinger, K. G., K. Keil, and T. E. Bunch
1967. Chromite from "Equilibrated" Chondrites. *American Mineralogist,* 52:1322–1331.

Steadman, R., and P. M. Nuttall
1963. Polymorphism in Cronstedite. *Acta Crystallographica,* 16:1–8.

Taylor, L. A., G. Kullerud, and W. B. Bryan
1971. Opaque Mineralogy and Textural Features of Apollo 12 Samples and Comparison with Apollo 11 Rocks. *Geochimica et Cosmochimica Acta,* Supplement, 2:855–871.

Turekian, K. K., and S. P. Clark
1969. Inhomogeneous Accumulation of the Earth from the Primitive Solar Nebula. *Earth and Planetary Science Letters,* 6:346–348.

Van Schmus, W. R.
1967. Polymict Structure of the Mezö-Madaras Chondrite. *Geochimica et Cosmochimica Acta,* 31:2027–2042.
1969. Mineralogy, Petrology, and Classification of Types 3 and 4 Carbonaceous Chondrites. Pages 480 to 491 in Millman, editor, *Meteorite Research.* Dordrecht, Holland: D. Reidel Publishing Company.

Watts, H. L.
1958. Volumetric Determination of Aluminum in Presence of Iron, Titanium, Calcium, Silicon and Other Impurities. *Analytical Chemistry,* 30:967.

Whipple, F. L.
1966. Chondrules: Suggestion Concerning the Origin. *Science,* 153:54–56.

Wood, J. A.
1963. On the Origin of Chondrules and Chondrites. *Icarus,* 2:152–180.
1967a. Olivine and Pyroxene Compositions in Type II Carbonaceous Chondrites. *Geochimica et Cosmochimica Acta,* 31:2095–2108.
1967b. Chondrites: Their Metallic Minerals, Thermal Histories, and Parent Planets. *Icarus,* 6:1–49.

☆ U. S. GOVERNMENT PRINTING OFFICE: 1973—516–221/14